

IMPACTS OF SINGLE-WALLED CARBON NANOTUBES ON POLYMERASE CHAIN REACTION

**A THESIS SUBMITTED TO
THE FACULTY OF ENGINEERING AND
NATURAL SCIENCES
OF
SABANCI UNIVERSITY**

BY

EBRU UYSAL

**IN PARTIAL FULFILMENT OF THE REQUIREMENTS FOR
THE DEGREE OF MASTER OF SCIENCES
IN**

**BIOLOGICAL SCIENCES AND BIOENGINEERING
DECEMBER 2014**

IMPACTS OF SINGLE-WALLED CARBON NANOTUBES ON POLYMERASE
CHAIN REACTION

APPROVED BY

Prof. Dr. Hikmet BUDAK

(Thesis Advisor)



Assoc. Prof. Levent ÖZTÜRK



Prof. Dr. Ersin GÖĞÜŞ



Dr. Meral YUCE

(Co-advisor)



APPROVAL DATE

16.01.2015

© EBRU UYSAL, 2014
All rights reserved

**IMPACTS OF SINGLE-WALLED CARBON NANOTUBES ON POLYMERASE
CHAIN REACTION**

EBRU UYSAL

Biological Sciences and Bioengineering, MS Thesis, 2014
Thesis Supervisor: Prof. Dr. Hikmet BUDAK

Keywords : Polymerase Chain Reaction, nanoPCR, Single-walled Carbon Nanotubes

ABSTRACT

Polymerase Chain Reaction (PCR) is an advanced technology used in modern era of molecular biology to amplify millions of copies of DNA from a single copy. In order to utilize this technique with its full potential, certain hindrances such as nonspecific by-products, low yield, complexity of GC rich and long genomic DNA amplification need to be eliminated. Among different PCR technologies, Nanomaterial-assisted PCR termed as nanoPCR is a developing technique used to get more improved and the most satisfactory results by using nanomaterials and PCR reaction together. Nanomaterials have been used in PCR due to their unique physical and chemical properties such as high thermal conductivity, stability and high surface to volume ratios that make them significant for numerous of research areas. The effects of nanomaterials in PCR depend on their size, shape, concentration, heat conductivity, electron transfer properties and surface modifications. Carbon nanotubes have hydrophobic surface area which make them tend to agglomerate into nanoropes in order to minimize surface energy and interaction with the environment.

In our study, the effect of Single-Walled Carbon Nanotubes (SWCNTs) was investigated in PCR in order to see their potential as next generation enhancers, where Polyacrylamide Gel Electrophoresis (PAGE), Dynamic Light Scattering (DLS) and Scanning Electron Microscopy (SEM) were mainly performed as core techniques. We demonstrated the impacts of three different SWCNTs in PCR; pristine, amine functionalized and carboxyl functionalized, at their different dispersion states including sonicated, centrifuged and filtered dispersions. The goal was to get rid of agglomerates formed during the reactions. The sonicated single-walled carbon nanotubes are long and have large aggregates as compared to centrifuged and filtered ones which are relatively smaller and short in size. Dynamic Light Scattering (DLS) is used to measure the relative hydrodynamic size of all three; sonicated, centrifuged and filtered single-walled carbon nanotubes to be employed in PCR. Our results

showed that intensities of electrophoretic bands of target DNA were affected by introduction of single-walled carbon nanotubes at different dispersion states and concentrations. This work would be useful in the complementary fields like nanobiology, nanomedicine and biosensing.

**TEK DUVARLI KARBON NANOTÜPLERİN POLİMERAZ ZİNCİR
REAKSİYONLARI ÜZERİNDEKİ ETKİLERİ**

EBRU UYSAL

Biyoloji Bilimleri ve Biyomühendislik, Yüksek Lisans Tezi, 2014
Tez Danışmanı: Prof. Dr. Hikmet BUDAK

**Anahtar Kelimeler: Polimeraz Zincir Reaksiyonu, nanoPCR, Tek Duvarlı Karbon
Nanotüpler**

ÖZET

Son zamanlarda, polimeraz zincir reaksiyonu tekniği nanoteknolojiden yarar sağlamaya başlamıştır. Bu tezde, Polimeraz Zincir Reaksiyonuna tek-duvarlı karbon nanotüplerin etkileri Polyacyrlamide Jel Elektroforez, Dinamik Işık Saçılma Teknikleri ve Taramalı Elektron Mikroskobu ile incelenmiştir. Kısa bir süre içinde düşük kopya sayısı, DNA'yı çoğaltmak üzere sağlayan in vitro Polimeraz Zincir Reaksiyonu (PCR) biyolojik çalışmaların ve tıbbın en önemli tekniklerden biri olmuştur. Tam potansiyeli ile bu tekniği kullanmak için, düşük verim ve zengin GC kontentine sahip uzun genomik DNA amplifikasyonun karmaşıklığı ve nonspesifik ürünlerin oluşumu gibi zorluklar ortadan kaldırılmalıdır.

Nano malzeme destekli PCR, nanoPCR olarak adlandırılır; geliştirilmiş ve nitelikli sonuçlar elde etmek PCR reaksiyonu ile nanoyapılı malzemelerin kombinlenmesi ile oluşan ve biyoteknolojide yeni gelişen bir alandır. Nano malzemeleri bu araştırma için önemli kılan hacim oranlarında yüksek ısı iletkenliği, stabilitesi ve yüksek bir yüzey olarak benzersiz fiziksel ve kimyasal özelliklere sahip olmalarıdır. PCR'da nanomateryallerin etkileri onların boyut, şekil, konsantrasyon, ısı iletkenliği, elektron transfer özellikleri ve yüzey modifikasyonlarına bağlıdır. Karbon nanotüpler topak oluşturmaya ve çevre yüzeyi ile etkileşim enerjisini en aza indirmeye eğilimli hidrofobik yüzey alanına sahiptir. Bu tezde, tek duvarlı karbon nanotüplerin PCR üzerindeki etkisi incelenecektir. Tek duvarlı karbon nanotüplerin büyük topaklanmalarının ortadan kaldırılması amacıyla deneylerde kullanılan karbon nanotüpler sonike edilmiş, sentrifuj edilmiş ve filtrelenmiş olacaklardır. Sonike edilmiş tek duvarlı karbon nanotüpler uzundurlar ve büyük topaklar vardır. Sonike edilmiş tek duvarlı karbon nanotüpler, sentrifüje tabi tutulur ve filtre edilir; bu örnekler sonike olanlara kıyasla daha küçük ve kısadırlar. Sonikasyona, sentrifüje ve filtreye tabi tutulan tek duvarlı karbon nanotüplerin görelî hidrodinamik boyutunu ölçmek amacıyla, dinamik ışık saçılımı

(DLS) kullanılır. Elde edilen sonuçlara göre, hedef DNA'nın elektroforetik bantlarının yoğunlukları incelenir. Karbon nanot plerin g rece hidrodinamik boyutları ve farklı konsantrasyon aralıklarında kullanımı, PCR'ı daha verimli hale getirir. Bu  alıřma nanobiyoloji, nanotıp ve biosens rleme gibi alanlarda tek duvarlı karbon nanot plere odaklanmış  alıřmaların geliştirilmesi i in uygundur.

in the great memory of Dr. Dicle Koğacioğlu

ACKNOWLEDGMENTS

I am extremely grateful to my supervisor Prof. Dr. Hikmet Budak for his guidance at all stages of my education life and all that I learned from him. Without his support, this thesis would not have been completed.

I would also like to thank my advisor Dr. Meral Yüce for her guidance and support through out my studies and final work. It is equally important to thank Dr. Hasan Kurt who supported my work with his precious advices and guidance. A very special thanks to TUBITAK and Sabanci University who supported me financially.

I must also present my gratitude to the weardy jury members: Assoc. Prof. Levent Öztürk and Prof. Dr. Ersin Göğüş for their patience, valuable advices and their contributions.

I have no words to thank my mother Sevim Uysal, father Op.Dr.Hüseyin Uysal, brother Op.Dr.Serkan Uysal and sister Dr.Eda Uysal who have always supported, encouraged and motivated me in all the sectors of my life. I am grateful for their guidance, endless love, care and their support in decision making process of my life.

I must also remember my cousin Tuğba Kara who is as closer to me as a sister for her support and being always there for me in my life.

I must not forget Mete Can Özbay for his help, support, encouragment and being a great friend. Thank you for being always there for me especially during my thesis period, for all ideas, patience and your time.

Last by no the least, I thank all my friends for being always there for me and their support and patience for me during my thesis period: Ahmet Eren Demirel, Aslıhan Demircan, Beste Bahçeci, Delfin Öztürk, Dilek Çakıroğlu, Emine Suer, Gizem Gezici, Havise Kavi, Işık Topak, İpek Özdemir, Naimat Ullah, Neslihan & Garbis Akçeoğlu.

TABLE OF CONTENTS

ABSTRACT	iv
ÖZET	vii
ACKNOWLEDGMENTS	x
1.Introduction	1
1.1. Polymerase Chain Reaction(PCR).....	1
1.2. Nanomaterial-assisted PCR (NanoPCR)	3
1.3. Carbon Nanotubes(CNTs)	4
1.4. Single-walled Carbon Nanotube-Asissted PCR	6
1.5. The Other Laboratory Techniques.....	12
2.Objective	14
3.Materials	15
3.1. Chemicals	15
4.Methods	16
4.1. Preparation of Single-walled Carbon Nanotubes Dispersions	16
4.2. UV-Visible Near Infrared (UV-Vis-NIR) Spectroscopy Measurements	16
4.3. Preparation of Amine functionalized Single-walled Carbon Nanotubes and Magnetic Beads.....	17
4.4. Scanning Electron Microscopy (SEM).....	18
4.5. Polymerase Chain Reaction(PCR).....	19
4.6. PCR Purification.....	19
4.7. Single-walled Carbon Nanotube-Assisted Polymerase Chain Reaction	20
4.8. Polyacrylamide Gel Electrophoresis(PAGE)	20
4.9. Dynamic Light Scattering(DLS)	21
5.Results	23
5.1. Preparation of Single-walled Carbon Nanotubes Dispersions	23
5.2. UV-Visible Near Infrared (UV-Vis-NIR) Spectroscopy Measurements	23
5.3. Preparation of Single-walled Carbon Nanotubes and Magnetic Beads.....	24
5.4. Dynamic Light scattering(DLS)	26
5.5. Polimerase Chain Reaction and Polyacrylamide Gel Electrophoresis	31
6.Discussion.....	36
7.Future Perspectives	38

8.Conclusion.....	40
9.References	42

LIST OF FIGURES

Figure 1.1	2
Figure 1.2	5
Figure 1.3.1	6
Figure 1.3.2	11
Figure 5.3.1	25
Figure 5.3.2	25
Figure 5.4.1	27
Figure 5.4.2	28
Figure 5.4.3	29
Figure 5.4.4	30
Figure 5.4.5	31
Figure 5.5.1	33
Figure 5.5.2	34
Figure 5.5.3	35
Figure 5.5.4	35

LIST OF TABLES

Table 1	3
Table 4.1	18
Table 5.3.1	24
Table 5.5.1	32
Table 5.5.2	32
Table 5.5.3	32

ABREVIATIONS

APS	Ammonium persulfate
°C	temperature in degrees Celsius
CNTs	Carbon Nanotubes
DLS	Dynamic Light Scattering
DNA	deoxyribonucleic acid
dNTP	deoxyribonucleotide triphosphate
EDC	1-ethyl-3-(3-dimethylaminopropyl) carbodiimide
EtBr	3, 8-diamino-5-Ethyl-6-phenyl phenanthridinium Bromide
MES	2-(<i>N</i> -morpholino)ethanesulfonic acid
MWCTs	Multi-Walled Carbon Nanotube
NHS	<i>N</i> -Hydroxysuccinimide
SWCNTs	Single-Walled Carbon nanotube
PCR	Polymerase Chain Reaction
rpm	rotations per minute
SEM	Scanning Electron Microscopy
PAGE	Polyacrylamide Gel Electrophoresis
TEMED	<i>N,N,N'',N''</i> -Tetramethylethylenediamine
μl	micro liter

1. Introduction

1.1. Polymerase Chain Reaction(PCR)

Polymerase Chain Reaction (PCR) was invented by Kary Mullis in 1985 who was rewarded with Nobel Prize later on in Chemistry in 1993.¹ Currently, PCR became common and inevitable for medical and biological researches with numerous of applications. It is used for *in vitro* amplification of multiple copies of specified fragments of DNA.² PCR is highly specific and sensitive for permitting copies of a sequences.³ PCR became common in laboratory research areas due to its availability and rapidness. The mechanism behind the PCR is based on knowing minimum sequence of DNA on either side of the region of DNA which is desired.⁴ There are complementary oligomers for these small regions that are situated for priming the amplification of the target sequence that are termed as primers.⁵

The procedure of PCR have repeated cycles which are heat denaturation, annealing and primer extension.⁶ On the heat denaturation step, DNA is untangled to become single stranded. The other step is annealing during which primers are hybridized specifically on their complementary sequences and with DNA polymerase enzyme, the primers are elongated by incorporating deoxynucleotides to create a newly synthesized complementary strand of DNA.⁷

Denaturation, annealing and extension are repeated as following cycles and on each cycle, the amplified strand is used as template for the next cycle. Thus, process becomes exponential amplification of DNA. To sum up, the following cycle of denaturation, annealing and extension by incorporating DNA polymerase, excess amount of primers and nucleotides are termed as PCR.⁸

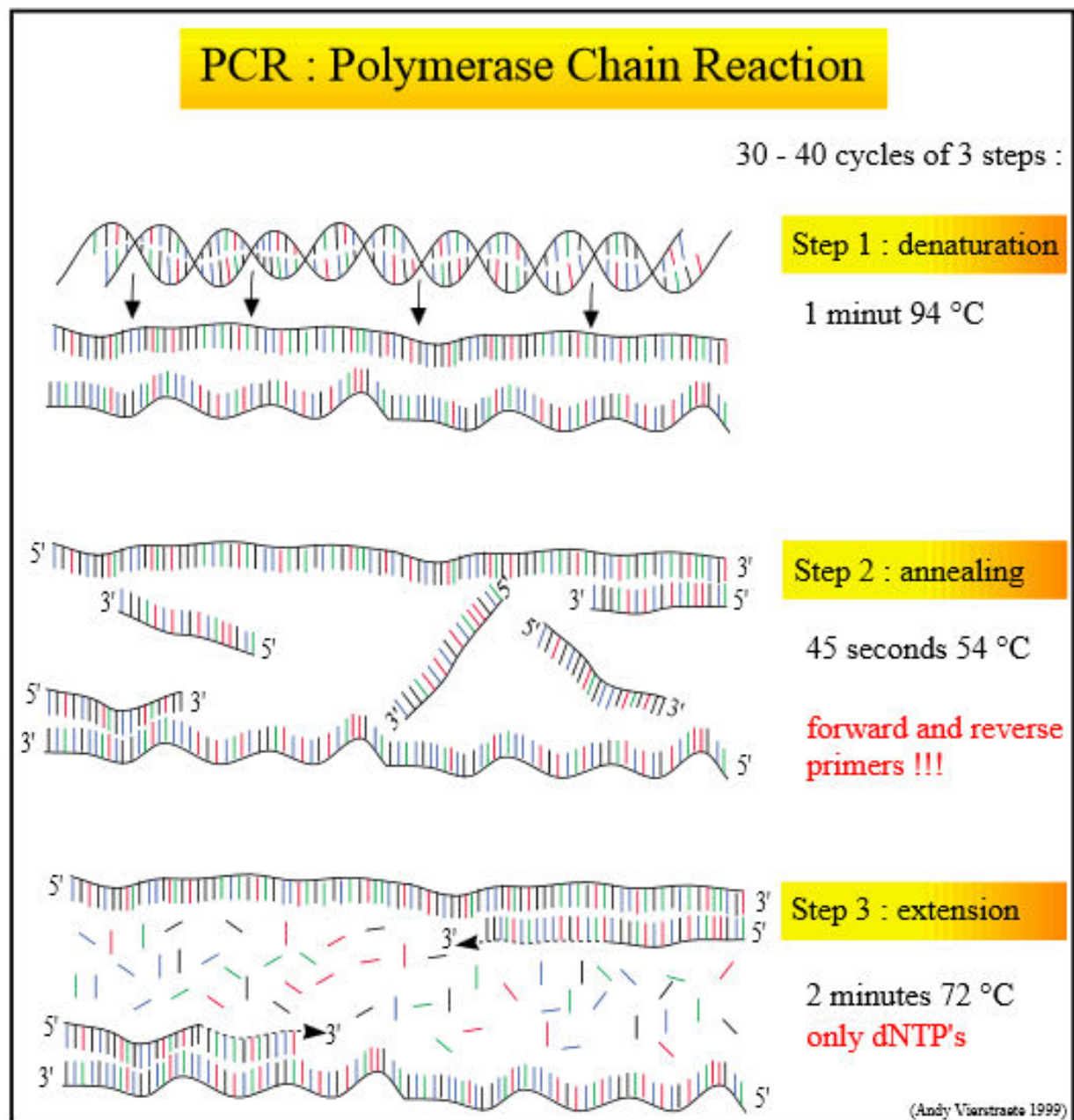


Figure 1.1 : Overview of PCR as steps of denaturation, annealing and extension.

Some of the applications of PCR are detecting infectious agents such as human immunodeficiency virus (HIV), diagnostics of cancer, detecting genetic disorders and paternity tests.⁹ The usage of PCR is increasing in many scientific research areas as molecular biology, microbiology, genetics, clinical diagnostics, forensic sciences, environmental sciences, hereditary researches, paternity testing and recently nanotechnology.¹⁰

In early PCR experiments, scientists had some difficulties on experiments. These difficulties are nonspecific PCR product, low yield and the difficulties of amplifying the DNA which has higher amount of GC content. To overcome these difficulties, scientists set useful guidelines. These guidelines are based on optimizing temperatures of steps, number of cycles, amount of primers, templates and enzymes, concentration of $MgCl_2$.¹¹ In order to obtain high quality results on PCR process should be manipulated.

Recently, a new field of research area arises that introduces nanomaterials into PCR reaction for developing the amount of PCR product and its specificity which is termed as Nanomaterial-assisted PCR or nanoPCR.¹²

1.2. Nanomaterial-assisted PCR (NanoPCR)

Nanomaterial-assisted PCR (NanoPCR) is a new area that is increasing and growing. It introduces nanomaterials into PCR reaction for developing the yield of PCR product and its specificity. Some of the nanostructured materials which are used as PCR components, are gold nanoparticles, graphene oxide, reduced graphene oxide, quantum dots, upconversion nanomaterials, fullerene, carbon nanotubes and other metallic nanoparticles.¹³ Among these nanomaterials, single-walled carbon nanotubes are focused on this work and a list of carbon nanotubes employed in PCR so far is provided in Table 1.

CNT	Size (nm)	CNT (mg/ml)	Impact	DNA (bp)	Enzyme	Mg (mM)	Ref.
SWCNT	2	<3	Increased efficiency	410	<i>Taq</i>	0-1.5	¹⁴
SWCNT	<2 10-20	0.05-0.8	Either reduced Efficiency or reaction inhibition	200	<i>Taq</i>	3	¹⁵
SWCNT-COOH							
MWCNT	1-2 <8	0.6-1.2 0.8-1.6	Increased efficiency and specificity,	14000	<i>Pfu, Taq</i>	2.8	¹⁶
MWCNT-COOH							
SWCNTs							
MWCNTs							

CNT-OH			unaffected fidelity				
CNT-COOH							
Negatively charged, pristine, acid-treated MWCNTs	30-70	2.3×10^{-2}	Increased efficiency and specificity	283	<i>Taq</i>	1.5	17
Positively charged Polyethyleneimine MWCNTs (CNT/PEI)	30-70	3.9×10^{-4}	Increased efficiency and specificity	283	<i>Taq</i>	1.5	17
Negatively charged Succinic anhydride CNT/PEI	30-70	6.3×10^{-1}	Increased efficiency and specificity	283	<i>Taq</i>	1.5	17
Neutral Acetic acid anhydride CNT/PEI	30-70	-	Slightly increased efficiency	283	<i>Taq</i>	1.5	17
Pristine PEI	-	4×10^{-5}	Increased efficiency and specificity	396	<i>Taq</i>	1.5	18
PDMS/MWCNTs based PCR system	20-70	-	Thermal conductivity induced reaction time improvement	150 756	<i>Taq</i>	0.25	19
CoMoCAT SWCNT (6,5)	0.8	0.01-1	Slightly increased efficiency	76	<i>Taq</i>	-	13

Table 1 : A list of carbon nanotubes recently employed in PCR.

1.3. Carbon Nanotubes(CNTs)

Carbon nanotubes are allotropes of carbon with a cylindrical shape of sp^2 -hybridized carbon atoms.²⁰ The name CNT is derived from its long, hollow structure with the walls formed by single atom-thick sheets of carbon, called grapheme.²¹ CNTs are constructed with a length-to-diameter ratio of up to 132,000,000:1, which is greater than any other standard material.²² Depending on their size in diameter, CNTs are categorized as single-walled carbon nanotubes (SWCNTs; 0.4–2 nm) and multi-walled carbon nanotubes (MWCNTs; 2–100 nm).²³ Characteristic properties of CNTs such as high electrical and thermal conductivity, high aspect ratios, exceptional mechanical strength and rigidity have given rise to their use in

a variety of applications including electrochemical energy storage and production,²⁴ field emission,²⁵ biosensor construction,²⁶ atomic force microscopy,²⁷ imaging²⁸ and DNA nanotechnology.¹² Among these, the discovery of DNA-assisted dispersion and separation of CNTs has opened up new avenues for CNT-based biotechnology research,^{29,30} one of which is addition of carbon nanotubes into biochemical reactions like PCR.

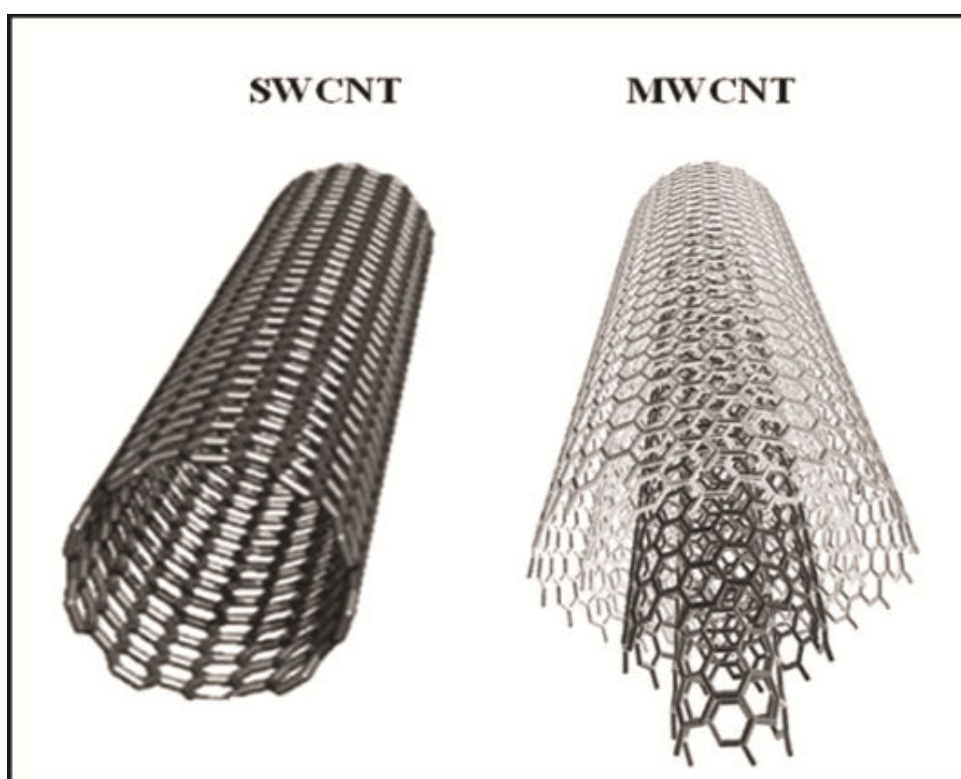


Figure 1.2 : Multi-walled & Single-walled Carbon Nanotubes, respectively.

Recently, new research area is emerged that combines biotechnology and nanomaterials. Under this fold, a new area that is named as bionanotechnology, biosensor technologies, biosensor construction, imagining, drug delivery and DNA nanotechnology can

be developed. Among these developments, single-walled carbonnanotube-assisted PCR is focused on this work.

1.4. Single-walled Carbon Nanotube-Asisted PCR

In general carbon nanotubes have large hydrophobic surface that promotes them to agglomerate into agglomerates for minimizing the surface energy and interaction with their environment. Due to decreased formation of agglomeration and bundles of carbon nanotubes, some functional groups as carboxyl and amine are introduced on the surfaces of carbon nanotubes. In this work, single-walled carbon nanotubes that have no functional group, carboxyl group and amine gruop functionalized carbon nanotubes are used for investigating their impacts on amplification of a random DNA library.

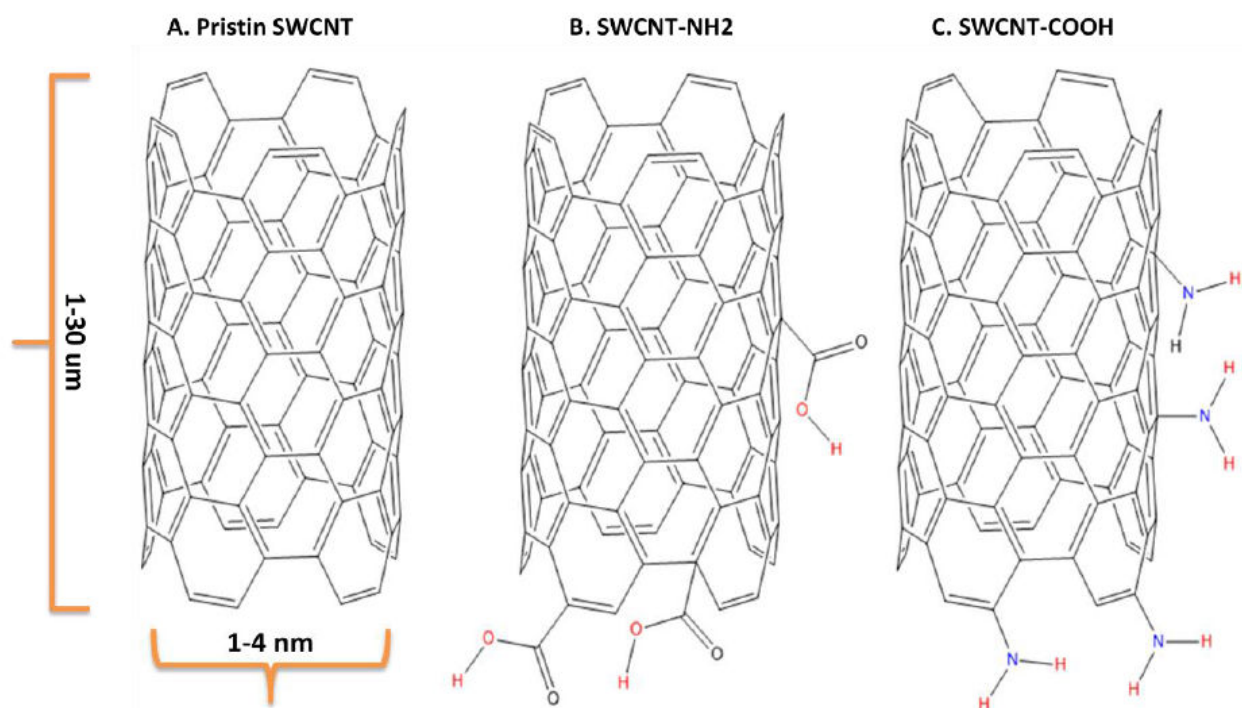


Figure 1.3.1 : Pristine, Amine functionalized and Carboxyl functionalized Single-walled Carbon Nanotubes, respectively.

First utilization of CNT in PCR has been reported by Cui et al.¹⁴, SWCNTs are promoted as PCR enhancers. According to the findings, the final yield of PCR product increased with the addition of SWCNTs up to 3 µg/ml, however the reaction was completely inhibited with increasing concentrations. Noticeably, the authors obtained similar results without including Mg²⁺ in the reaction, which is an essential cofactor for DNA polymerase enzyme to maintain its activity. Although High Resolution Transmission Electron Microscopy (HRTEM) and X-Ray Photoelectron Spectroscopy (XPS) data implied a potential physical interaction between SWCNTs and PCR components, the underlying reason of such interaction might be merely the solvent evaporation effect. Since water has a considerable amount of surface tension energy, the liquid–gas interface can carry particles into a limited space during its evaporation. Eventually, free components of sample would tend to concentrate on the first surface available^{31,32}. Therefore, interactions at bio-nano interface should be further investigated by the techniques that allow to assess materials in their native environment, such as Circular Dichroism (CD) spectroscopy, In situ Atomic Force Microscopy (AFM) and Nuclear Magnetic Resonance Spectroscopy (NMR).

In another study conducted by Zhang et al.¹⁶ improved PCR efficiency and specificity by incorporation of CNTs has been reported where a long 14.3kb lambda DNA was used as template. After performing PCR containing different types of carbon-based nanomaterials (carbon nanopowder, SWCNTs and MWCNTs with different size and surface properties) at various concentrations (max 1 mg/ml) it is found that all the tested nanomaterials increased the efficiency and specificity of PCR with a CNT concentration of approximately 0.8 mg/ml. To assess the fidelity of the CNT-assisted PCR, Zhang et al.¹⁶ evaluated Sanger sequencing data of CNT-free PCR and CNT-assisted PCR (SWCNT and MWCNT). The preliminary results showed no significant drop in DNA replication fidelity in comparison to the

conventional PCR. Additionally, Shen et al.³³ found the error rates of control PCR, SWCNT and MWCNT assisted PCR as 5.26×10^{-6} , 16.25×10^{-6} and 32×10^{-6} , respectively, which was better than the error rate of betaine (69×10^{-6}). Despite the fact that the current fidelity results are not sufficient enough to prove CNT as a viable PCR additive, the data is still promising for further investigation of CNTs in PCR.

There are a large number of reports proving the exceptional thermal³⁴ and mechanical³⁵ properties of CNTs, however, there is still lack of information on the impact of these parameters in PCR which is already a heat-transfer technique. It has been reported that thermal conductivity of individual SWCNTs (9.8 nm in diameter) measured at room temperature surpasses 2000 W/mK and increases as its size decreases in diameter³⁶. Although the thermal conductivity of bulk CNTs is lower than SWCNTs, the minimum thermal conductivity is still significantly higher than pure water (0.6 W/mK at 20 °C)³⁷. This information proposes that CNT-containing PCR suspension would have a higher thermal conductivity and thus could provide a better thermal transfer and heat equilibrium in PCR tubes. Based on this assumption, Quaglio et al.¹⁹ introduced metallic MWCNTs into Poly (Dimethyl) Siloxane (PDMS/CNTs) to monitor alteration in PCR efficiency originating from only thermal properties of the nanocomposite. In the experiment, nanocomposite is deposited on a chip based PCR system and blocking the surface with Bovine Serum Albumin (BSA) prevented surface effect of CNTs. The results displayed a considerable reduction in total reaction time by 75% demonstrating the direct advantage of the MWCNTs in the nanocomposite. Consistent with that result, Cao et al.¹⁷ obtained improved PCR products at varying annealing temperatures between 30-55 °C, in which improvement has also been affected by different surface charges of polyethyleneimine-modified MWCNTs.

As presented in Figure 1.3.2, both negatively-charged MWCNTs (acid-treated pristine MWCNTs and succinic anhydride-modified CNT/PEI) and positively charged MWCNTs (CNT/PEI) improved the efficiency and specificity of PCR with optimum concentrations of 2.3×10^{-2} and 6.3×10^{-1} mg/ml, respectively. Nevertheless, neutral MWCNTs (acetic anhydride modified-CNT/PEI) showed neither improvement nor inhibition under similar conditions.

These observations suggest that the mechanism of CNT-assisted PCR cannot be thoroughly explained with improved heat conductivity since other factors such as surface charge and electrostatic interactions between nanomaterial and PCR components also contribute to PCR enhancement. In order to probe the physical interaction between MWCNTs and PCR reagents, major PCR components; primers, template (283bp) and DNA polymerase (recombinant) are individually incubated with negatively-charged acid-treated pristine MWCNT at a concentration of 12.4 mg/ml and then combined with remaining PCR reagents prior to thermal cycling¹⁷.

It has been discovered that incubation of primers and DNA polymerase with MWCNTs prior to thermal cycling decreases the efficiency of PCR slightly as a result of restricted interaction of the template with primers and the enzyme. It should be noted that the type of polymerases (recombinant, mutant, *Taq*, *Pfu* polymerase), primers, length and sequence of templates and physical properties of CNTs vary from one study to another, so owing to their unique structures they might exhibit different behaviors when they are interacted with CNTs.

For instance, in contradiction to previous findings, Yi et al.¹⁵ reported that CNTs (SWCNT, SWCNT-COOH, MWCNT and MWCNT-COOH) either reduced or inhibited the PCR reactions where the inhibitory effect increased in the order of CNT-COOH > Pristine

CNT and SWCNT > MWCNT. In order to discover the source of inhibition, authors surveyed the interaction between CNTs and wild type *Taq* DNA polymerase by incubating the enzyme with different types of CNTs at various thermal conditions. The data obtained revealed the adsorption of *Taq* DNA polymerase onto the CNTs regardless of their surface charges or functional groups. Interestingly, it has been also stated that the adsorbed enzyme maintained its activity during PCR, which was evident with target bands on agarose gel.

In agreement with this result, Williams et al.¹³ reported that the adsorption of *Taq* DNA polymerase on SWCNT is unlikely to inhibit PCR reaction. Eventually, inhibition of the reaction is anticipated as nanomaterial-induced formation of free radicals. There is however no direct experimental evidence of oxidative stress caused by CNT-derived free radicals,³⁸ on the contrary, MWCNTs are shown to have a significant radical scavenging capacity.³⁹ From a different point of view, if the enzyme were still active after adsorption, the reduced band intensities of the targets would be explained with the adsorption of amplified DNA onto CNTs, which would gradually prevent their visibility on the gel at increasing concentrations. To prove such an adsorption of the amplified DNA, purified PCR products could be subjected to thermal cycle with CNTs at different concentrations and evaluated on a high-resolution gel (for example native polyacrylamide gel) under similar conditions. Additionally, the presence of large CNT bundles and the formation of the new bundles during thermal cycles could be other reasons for such inhibition, which may be eliminated or reduced by advanced probe-sonication and filtration steps.

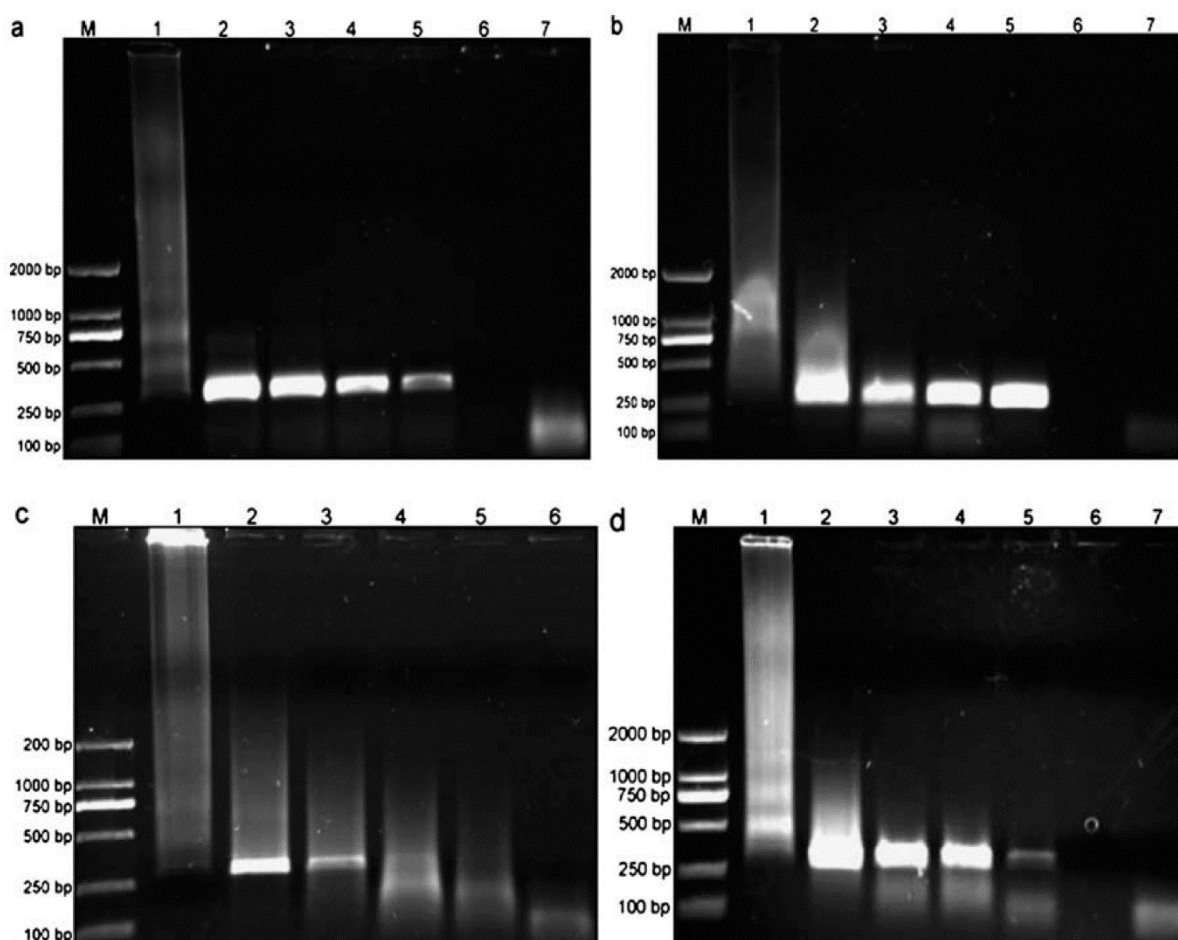


Figure 1.3.2: The effect of different surface charges on CNT-assisted PCR. First lane is marker and last lane is negative control **a)** Negatively charged acid-treated pristine MWCNT, from lane 1 to 6, the final concentrations are 0, 15.52, 23.28, 31.04, 38.80, and 46.56 mg/L, **b)** Positively charged PEI-modified MWCNT, from lane 1 to 6, the final concentrations are 0, 0.17, 0.22, 0.28, 0.39, and 0.44 mg/L, **c)** Neutral CNT/PEI modified with acetic anhydride, from lane 1 to 5, the final concentrations are 0, 6.19, 18.57, 30.95, and 43.34 mg/L, **d)** Negatively charged CNT/PEI modified with succinic anhydride, from lane 1 to 6, the final concentrations are 0, 0.54, 0.63, 0.78, 0.82, and 0.86 g/L, respectively. Reproduced with permission from Ref: ¹⁷ Copyright © 2009

Wiley-VCH Verlag GmbH & Co. KGaA, Weinheim.

1.5. The Other Laboratory Techniques

PCR purification, Polyacrylamide Gel Electrophoresis(PAGE), Dynamic Light Scattering(DLS), Scanning Electron Microscopy(SEM) techniques are used in this study. The most focused and the main technique are PCR and nanoPCR that have carbon nanotube additives. PAGE is used for visualizing the yield of PCR as band intensities. DLS and SEM are implemented for surface morphology and characterization.

Agarose gel is generally used to visualize PCR bands. However, in this work polyacrylamide gel electrophoresis is used instead of agarose gel. Agarose gel is appropriate for resolving nucleic acid fragments that are around 10-15 kb as size. Below this range, it is difficult to separate and visualize because in the gel matrix there is diffusion. On native polyacrylamide gel, fragments that are as small as 10 bp can be separated since it provides high resolution. Native PAGE has the advantage of having high loading capacity in a single well thus separating small fragments effectively.

Native Polyacrylamide gel is formed by polymerization of acrylamide monomers into long chains that are covalently attached by a cross-link agent as bisacrylamide and they both break down in solution to acrylic acid that have impacts on mobility of the molecules through the gel matrix. Ammonium persulfate (APS) is used to initiate the reaction which is further stabilized by TEMED. For native PAGE, the pore size is significant and is determined by the percentage expression of total acrylamide. There is an inverse proportion between pore size and percentage of the acrylamide which means as the percentage of the gel increases, the pore size decreases. For the successful separation of DNA fragments, polymerization of gel and percentage of acrylamide are significant.⁴⁰

DLS technique was used to measure hydrodynamic size distribution of the NH₂-MWCNT dispersions. Malvern Zetasizer Nano ZS was equipped with a vertically polarized He–Ne laser (633 nm) operating at 173° (Malvern Instruments, ZEN3600, UK). DLS technique provides a hydrodynamic size distribution calculated via the Stokes-Einstein equation from the dynamic fluctuations of light scattering intensity which is generated from Brownian motion of the spherical particles. Although DLS technique assumes particles as perfect spheres, it still could provide valuable information for CNT's hydrodynamic size distribution as previously reported^{41–45}, based on CNT length and diameter by using the following equations:

Translational diffusion coefficient (D_t) of a CNT or any other cylindrical structure⁴⁶ is:

$$D_t = \frac{kT}{3\pi\eta L} \left[\ln \left(\frac{L}{d} \right) + 0.32 \right]$$

Where k is the Boltzmann's constant, T is temperature of the medium, η is the viscosity of the medium, L is the CNT length and d is the CNT diameter. We can introduce this equation into the Stokes-Einstein relationship, which DLS technique utilizes to deduce hydrodynamic diameter (D_h) from the translation diffusion coefficient, D_t

$$D_t = \frac{kT}{3\pi\eta D_h} ; D_h = \frac{L}{\ln(L/d) + 0.32}$$

2. Objective

The aim of this thesis is to investigate the impacts of pristine, amine and carboxyl functionalized single-walled carbon nanotubes on PCR which is for randomized DNA library. In addition to that, interaction between SWCNTs and major PCR components are also explored.

The motivation for this work is observing the increase or decrease on the efficiency of PCR products in the presence of pristine, SWCNT-NH₂ and SWCNT-COOH. For this work PCR, polyacrylamide gel electrophoresis, dynamic light scattering(DLS), UV-Vis-NIR spectroscopy and scanning electron microscopy(SEM) techniques are used.

Challenges are faced during the working with single-walled carbon nanotubes that can get easily agglomerated. During PCR, SWCNTs are agglomerated at the bottom of the PCR tubes which is the difficulty of that study. Due to agglomerated SWCNTs, it was unable to declare that the bands that are visualized are desired PCR product. Thus, on this work sonicated, centrifuged and filtered SWCNTs are used to observe the difference between the samples that contain larger agglomerates and the samples contain smaller agglomerates.

There is possibility that SWCNTs can bind major PCR components as template, Taq polymerase enzyme, forward primer and reverse primer. The main hurdle of this work is visualizing primer dimers which is by-product of PCR.

On the other hand, SWCNTs are used as PCR enhancers which makes the work efficient. This work will be efficient for the future applications focusing on exploitation on SWCNTs biological systems as nanobiology, nanomedicine and so on.

3. Materials

3.1. Chemicals

Pristine, amine functionalized and carboxyl functionalized single-walled carbon nanotubes were purchased from Graphene Chemical Industries Co.(Ankara, Turkey). PCR reagents are purchased from KAPA Biosystems Co. (Catalogue no: KK1008, Woburn, MA, USA). 30% Acrylamide/Bis Solution, 29:1, Tetramethylethylenediamine (TEMED) and Ammonium persulfate (APS) were purchased from Sigma-Aldrich (St. Louis, MA, USA).

All glasswares, PCR tubes, eppendorfs and pipet tips were autoclaved by using Hirayama autoclave (Che Scientific Co., Hong Kong). In addition,, 5x PCR Buffer and 10x TBE Buffers were prepared in our lab and autoclaved. For 5x PCR Buffer, 10x PCR Buffer was prepared in our laboratory as mixing 500 mM KCl, 100 mM Tris-HCl pH 8.3 and 1% Triton X-100 and from 10x PCR Buffer, 5x and 1x PCR buffer is obtained as diluting.

4. Methods

4.1. Preparation of Single-walled Carbon Nanotubes Dispersions

Single-walled carbon nanotubes were purchased as powder and they were resuspended in autoclaved Milli-Q water at 1 mg/mL final concentration. Tween 20 which is nonionic detergent was used as dispersion agent that is for making dispersion process easier Tween 20 is used 0.1% at final concentration.

Sonication was performed at room temperature on ice by using microtip probe at 35% amplitude for 1 hour with 10 seconds pulse on and 15 seconds pulse off. After sonication, four 1.5 ml eppendorf tubes of single-walled carbon nanotubes were taken and centrifuged at 14000 rpm for half an hour. Following the centrifugation process, supernatant of single-walled carbon nanotubes were taken and 250 μ l from bottom of the tubes was discarded. This step was repeated for two times. The aim of the centrifugation and discarding the bottom was to eliminate the bigger aggregates. Finally, two centrifuged eppendorf tubes from four tubes were filtered with Millipore Polycarbonate Syringe 0.2 μ m filteres with the aim to eliminate the bigger agglomerates and acquire smaller dimensioned nanotubes.

4.2. UV-Visible Near Infrared (UV-Vis-NIR) Spectroscopy Measurements

The absorbance of single-walled carbon nanotubes was measured by using Varian Model Carry 5000 UV-Visible-Near-Infrared Spectroscopy (Agilent Instruments, USA). The samples were prepared at different concentrations of single-walle carbon nanotubes were suspended in autoclaved Milli-Q water that included 0.1% Tween 20. Absorbance was measured with Quartz Cuvettes with a light path of 10 mm and volume with 700 μ l. As a

reference, Milli-Q water including 0.1% Tween 20 that is only surfactant, was measured to subtract from the samples which included single-walled carbon nanotubes at different concentrations.

4.3. Preparation of Amine functionalized Single-walled Carbon Nanotubes and Magnetic Beads

To visualize binding interactions between single-walled carbon nanotubes and major PCR components as DNA template, DNA polymerase enzyme and primers, magnetic beads were prepared. The prepared magnetic beads were interacted with single-walled carbon nanotubes.

25 μ l carboxylic acid functionalized magnetic bead that is used for amine functionalized single-walled carbon nanotubes is taken from main stock which had concentration of 10mg/ml. The supernatant of magnetic bead was taken by using magnetic stand. Magnetic beads were washed with 25 mM MES Buffer (pH 5.5) for five times and supernatant was removed. The ligand is dissolved in MES Buffer and 300 μ l of newly sonicated and centrifuged 300 μ l carboxyl functionalized single-walled carbon nanotubes were added.

Independently from these processes, 10 mg 1-Ethyl-3-(3-dimethylaminopropyl) carbodiimide (EDC) was dissolved in 1 ml autoclaved Milli-Q water and 10 mg *N*-Hydroxysuccinimide (NHS) was dissolved in 1 ml autoclaved Milli-Q water. 100 μ l EDC and 100 μ l NHS was mixed together and well vortexed.

Five 1.5 ml eppendorf tubes were prepared that included different concentration of single-walled carbon nanotubes. The ingredients of the tubes can be seen on the table below.

	Eppendorf 1	Eppendorf 2	Eppendorf 3	Eppendorf 4	Eppendorf 5
Amine Functionalized SWCT	25 μ l	50 μ l	75 μ l	100 μ l	125 μ l
Carboxyl Functionalized Magnetic Beads	50 μ l	50 μ l	50 μ l	50 μ l	50 μ l
MES Buffer (pH 5.5)	105 μ l	80 μ l	55 μ l	30 μ l	5 μ l
EDC-NHS	20 μ l	20 μ l	20 μ l	20 μ l	20 μ l

Table 4.1: The different concentrated of single-walled carbon nanotubes for preparation of magnetic beads.

These five 1.5 ml eppendorf tubes that included different concentration of amine functionalized single-walled carbon nanotubes and carboxyl functionalized magnetic beads, EDC-NHS and MES Buffer were mixed well and shaken overnight at room temperature.

Beads were washed for three times with 150 μ l MES Buffer and three times with 150 μ l Milli-Q water including 0.1 % Tween 20 and three times with 175 μ l Milli-Q water. To eliminate the unbound single-walled carbon nanotubes from the incubated media, washing steps with MES Buffer, Milli-Q water including 0.1 % Tween 20 and Milli-Q water was performed.

Finally, amine functionalized single-walled carbon nanotubes and carboxyl functionalized magnetic beads were resuspended in 400 μ l autoclaved Milli-Q water.

4.4. Scanning Electron Microscopy (SEM)

To prove whether to visualize the beads were covered with single-walled carbon nanotubes or not, Scanning Electron Microscopy (LEO Supra 35 VP Field Emission SEM) was used. For Scanning Electron Micsocopy visualization, 1 μ l of samples are dropped on

clean Silicon Wafers, dried for four hours at room temperature and dried by vacuum before visualizing.

4.5. Polymerase Chain Reaction(PCR)

94mer random DNA oligonucleotide library and the primers were purchased from Microsynth (Microsynth GmbH, Balgach, Switzerland). The random oligonucleotide library includes 50mer random region flanked by fixed and known primer binding sites at 5' and 3' end (**5'-AGCTCCAGAAGATAAATTACAGG N50 CAACTAGGATACTATGACCCC-3'**). The random oligonucleotide library was amplified using a protocol as 25 µl of reaction mixture which contained 1U of KAPA Taq Polymerase enzyme, 2.5 µl of KAPA 10x PCR Buffer A, 0.5 10 mM dNTPs mixture, 1 µl 25 mM MgCl₂, 20 µl autoclaved Milli-Q water, 0.5 µl 30 ng/µl single stranded DNA template, 0.5 µl 160 ng/µl Forward Primer and 0.5 µl Reverse Primer.

4.6. PCR Purification

In order to clean double-stranded DNA from the excess of primers, salts and dNTPs; 20 tubes of PCR reaction were prepared as 25 µl of reaction mixture which contains 1U of KAPA Taq Polymerase enzyme, 2.5 µl of KAPA 10x PCR Buffer A, 0.5 10 mM dNTPs mixture, 1 µl 25 mM MgCl₂, 20 µl autoclaved Milli-Q water, 0.5 µl 30 ng/µl single stranded DNA template, 0.5 µl 160 ng/µl Forward Primer and 0.5 µl Reverse Primer. All PCR products were mixed together and divided into two 1.5 ml eppendorf tubes as 250 µl pf PCR products. 125 µl 5M ammonium acetate was added on the PCR product mixed and vortexed well for 30 seconds. 375 µl of absolute ethanol was added and mixed well, finally vortexed for 30 seconds. Samples were incubated at -80 °C for overnight to get frozen. At 14 000 rpm for 1 hour, samples were centrifuged for 14,000 RPM, 1 hour at 4 °C Supernatant of the

samples was taken and suspended in 35 μ l autoclaved Milli-Q water and the sample were incubated at 45 °C on the hot block to evaporate ethanol for an hour.

At the end of the PCR purification, concentration was measured as 1 μ l on nanodrop and diluted till 30 ng/ μ l.

4.7. Single-walled Carbon Nanotube-Assisted Polymerase Chain Reaction

Single-walled carbon nanotubes were added as PCR components into the reaction tube. Firstly, single-walled carbon nanotubes were added in PCR tubes at different concentration by performing serial dilution with water. Master mix was prepared and separated into each PCR tubes with total volume 25 μ l. PCR protocol used was 3 min at 95 °C followed by 8 cycles of 20 seconds at 95 °C, 20 seconds at 58 °C and 20 seconds at 72 °C. A final extension step at 72 °C for 1 min. PCR is performed by using Master Cycler Gradient 384 (Eppendorf, NY, USA).

4.8. Polyacrylamide Gel Electrophoresis(PAGE)

After PCR, samples that included single-walled carbon nanotubes were spun down for one minute on a bench-top mini centrifuge and supernatants were loaded on gel. Two pieces of 6% native polyacrylamide gel was prepared by mixing 3 ml 30% Acrylamide/Bis Solution (29:1), 3 ml 5x TBE, 7 ml autoclaved Milli-Q water, 20 μ l Tetramethylethylenediamine (TEMED) and 200 μ l Ammonium persulfate (APS). 5x TBE was diluted from 10x TBE buffer that was prepared as main stock in our laboratory. For 1 ml 10x TBE Buffer, 108 g Tris-base, 55 g Boric acid and 40 ml 0.5 M pH 8 EDTA were dissolved in 800 ml distilled water. Buffer was left on stirrer overnight at 60°C. 5x TBE

Buffer was prepared by diluting with half amount of water and half amount of 10x TBE stock buffer.

5 μ l sample which was taken from top of the PCR tube and 1 μ l 6x loading dye was mixed well on parafilm and loaded per each well as 5 μ l. Gel was runned at 100 volts for 65 minutes in BioRad Mini Protean Cells (Biorad, Hercules, Ca) that is filled with 5x TBE Buffer as running buffer.

For visualizing, gel was stained with 10 mg/ml Ethidium Bromide solution which is prepared by resuspending 50 μ l Ethidium Bromide in 500 ml 5x TBE Buffer. After running has been finished, the gel was stained with Ethidium Bromide solution for one minute and washed with autoclaved Milli-Q water for 1 minute. DNA bands were visualized under BioRad GelDoc EZ Digital Systems (Biorad, Hercules, Ca).

Gel images were analyzed by using ImageJ software that is based on the black and white color intensities in pixels of the bands and the background of the bands.

4.9. Dynamic Light Scattering(DLS)

1x PCR Buffer was prepared for sample preparation to measure. 1x PCR Buffer was diluted from 10x PCR Buffer that was prepared as main stock. For 50 ml 10x PCR Buffer, 25 ml of 1M KCl, 5 ml of 1M Tris-HCl, 0.5 ml of Triton X-100, 19.5 ml of water and 100 μ l 25mM of $MgCl_2$ were mixed together. The well mixed 10x PCR Buffer was filtered with Millipore Polycarbonate Syringe 0.2 μ m filter to make the solution pure.

Samples were prepared by diluting in 1x PCR Buffer by thousand folds and transferred into the quartz DLS Cuvettes which were square cell with 12mm O.D. (Malvern, Germany).

Dynamic Light Scattering is used for measuring the hydrodynamic radius of single-walled carbon nanotube dispersions. The machine, Malvern Zetasizer is programmed as vertically polarized He-Ne laser at 633 nm operating at 173° (Malvern Instruments, ZEN 3600, UK).

Data collecting was performed by using NLS algorithm that uses 45 measurement cycles for each sample and each independent measurement is repeated as 15 scans.

Temperature studies were performed due to thermal changes under PCR machine, changes are set from 20 °C to 90 °C with 5 °C increment which included all temperatures of polymerase chain reaction.

Samples were equilibrated for five minutes before each temperature point. On the software of Zetasizer results were given as the average and standard deviation from at least three measurements.

5. Results

5.1. Preparation of Single-walled Carbon Nanotubes Dispersions

The powdered single-walled carbon nanotubes were resuspended in Milli-Q water including 1% Tween 20 were sonicated at room temperature on ice by using microtip probe at 35% amplitude for 1 hour with 10 seconds pulse on and 15 seconds pulse off. This process was performed on ice to decrease the risk of bundles. The biggest problem about working with carbon nanotubes is agglomeration. To remove the bigger agglomerated carbon nanotubes, centrifugation was performed.

We used pristine that has no functional group, SWCNT-NH₂ and SWCNT-COOH. All of them were prepared and sonicated at the same conditions. However, the sonication of pristine took more time and was difficult in comparison to the others. The sonication duration speed ranking is SWCNT-NH₂>SWCNT-COOH>Pristine. The functional groups had impacts of dispersity.

5.2. UV-Visible Near Infrared (UV-Vis-NIR) Spectroscopy Measurements

Varian model Carry 5000 UV-Vis-NIR Spectrophotometer (Agilent Instruments, USA) was used to measure absorbance of the prepared SWCNT dispersions. All samples were diluted by thousand fold with sterile Milli-Q water containing Tween 20 at 0.1% final concentration, and scanned in quartz cuvettes between 200-1200 nm with 1 nm intervals. The Milli-Q water including only the surfactant at 0.1% final concentration was used as reference, in which the absorbance values of this sample was subtracted from the absorbance of the SWCNT samples. The final SWCNT concentrations of the samples were calculated applying

the Lambert–Beer law: $A = \epsilon.C.L$, where A is the absorbance at a given wavelength, C is the SWCNT dispersion concentration (mg mL^{-1}), ϵ is the effective extinction coefficient and L is the optical pathway, which is given by the length of the quartz cuvette (1 cm). The absorbance values of 500 nm for SWCNT-P⁴⁷, 850 nm for SWCNT-NH₂⁴⁸ and 1025 nm for SWCNT-COOH⁴⁹ were used along with the extinction coefficient values of $30.5 \text{ mL.cm}^{-1}.\text{mg}^{-1}$, 7.9 and $12.8 \text{ L.g}^{-1}.\text{cm}^{-1}$, respectively.

5.3. Preparation of Single-walled Carbon Nanotubes and Magnetic Beads

To observe binding interactions between single-walled carbon nanotubes and major PCR components as DNA template, DNA polymerase enzyme and primers, magnetic beads are prepared. The prepared magnetic beads were interacted with single-walled carbon nanotubes. Magnetic beads and SWCNT-NH₂ were covalently bounded to each other with EDC-NHS crosslinking that is the process of chemically binding of more than two molecules by covalent bonds.

	Eppendorf 1	Eppendorf 2	Eppendorf 3	Eppendorf 4	Eppendorf 5
Amine Functionalized SWCT	25 μl	50 μl	75 μl	100 μl	125 μl
Carboxyl Functionalized Magnetic Beads	50 μl	50 μl	50 μl	50 μl	50 μl
MES Buffer (pH 5.5)	105 μl	80 μl	55 μl	30 μl	5 μl
EDC-NHS	20 μl	20 μl	20 μl	20 μl	20 μl

Table 5.3.1 : The different concentrated of single-walled carbon nanotubes for preparation of magnetic beads.

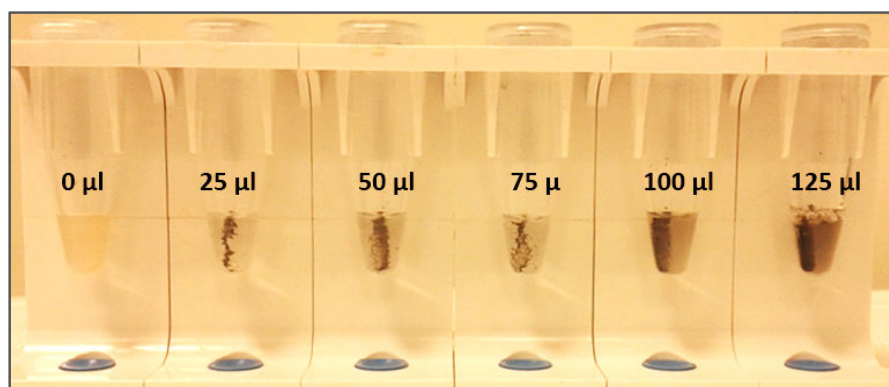


Figure 5.3.1: Preparation of magnetic beads that are covered with SWCNT-NH₂

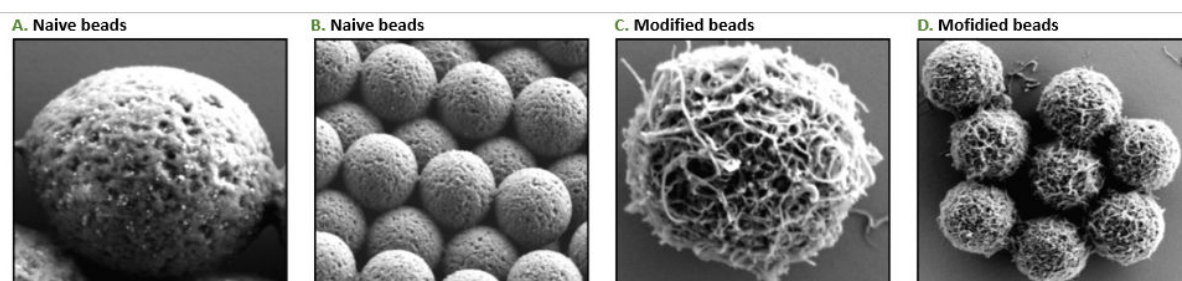


Figure 5.3.2: SEM micrographs of the Naïve (A and B) and SWCNT-NH₂ modified magnetic beads (C and D).

Beads were washed for three times with 150 µl MES Buffer and three times with 150 µl Milli-Q water including 0.1 % Tween 20 and three times with 175 µl Milli-Q water.

After washing step 1 µl of samples were dropped on clean Silicon Wafers, dried for four hours at room temperature and dried by vacuum before visualizing. Whether to visualize the beads are covered with single-walled carbon nanotubes or uncovered Scanning Electron Microscopy (LEO Supra 35 VP Field Emission SEM) is used.

For SEM visualization, Dr.Hasan Kurt is expertized for this work. The results are not at the high quality. Single-walled carbon nanotubes are smaller than salts which the buffer of

magnetic beads have. Thus, SWCNTs are not observed. The bigger salts are visualized under the SEM. In addition to that, at the step of preparing magnetic beads which are covered with SWCNTs the binding can be observed with bare eye. On the Figure 5.3.1., there are eppendorfs are seen and in these eppendorfs carbon nanotubes are seen as black. If the magnetic beads and SWCNTs are bounded successfully they can be seen as brownish colour.

5.4. Dynamic Light scattering(DLS)

Carbon nanotubes have the propensity to self-agglomerate into larger bundles and ropes with strong van der Waals interaction energy (ca. 500 eV/ μm of tube contact)⁵⁰ which makes the carbon nanotube dispersion a challenging task. It is known that dispersion quality, aggregate size, polydispersity and morphology of the carbon nanotubes affects their mechanical and electrical properties as well as biological activities.⁵¹ In the current study, a) sonicated, b) sonicated and centrifuged, c) sonicated, centrifuged and filtered water dispersions of SWCNT-P, SWCNT-NH₂ and SWCNT-COOH produced via CVD method were tested in the PCR amplification of two different DNA templates in order to understand the impact of dispersion states and surface charges in the final amplification yield of the templates. To evaluate the relative size distribution of the prepared SWCNT dispersions, we used the DLS technique based on the Stokes-Einstein equation^{52–55} and the UV-Vis-NIR spectrophotometry technique for the actual concentration measurements. Figure 5.4.1 shows the influence of centrifugation and filtration steps on removing the big CNT aggregates and bundles from the sonicated dispersions. The relative hydrodynamic size distribution of SWCNT-P and SWCNT-COOH dispersions sharply decreased from thousand to hundreds nanometers following the centrifugation step and a moderate intensity change was observed after the membrane filtration. On the other hand, sonicated SWCNT-NH₂ dispersion presented

a uniform size distribution between 100-500 nm, which replaced with smaller agglomerates around 220 nm and 190 nm after the centrifugation and filtration steps, respectively. The Z-average hydrodynamic diameters of the samples with polydispersity indexes were provided in SI.

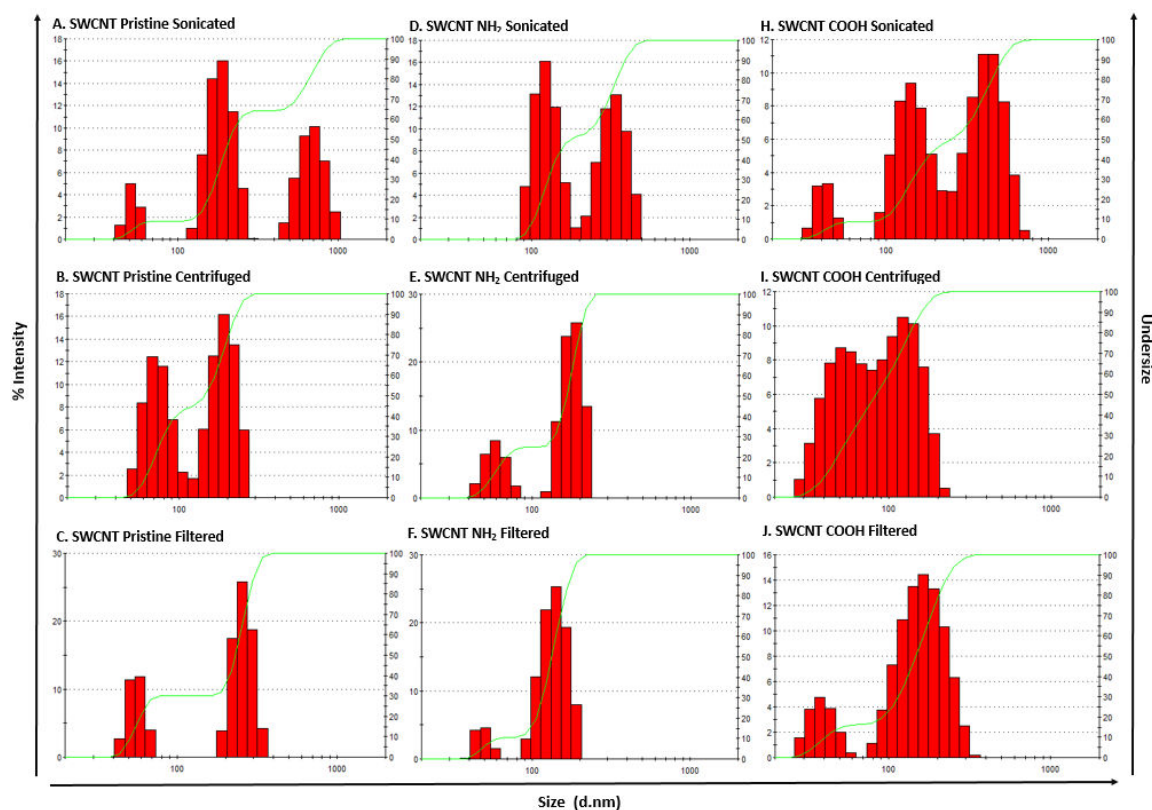


Figure 5.4.1 : Variation in relative hydrodynamic size distribution of the SWCNT-P (A), SWCNT-NH₂ (D) and SWCNT-COOH dispersions (H) upon centrifugation (B, E, I) and membrane filtration (C, F, J). The data shows the collective result of three different measurements for each SWCNT dispersion. The concentrations of the SWCNT dispersions calculated from Beer-Lambert equation were found to be 137, 54, 27 $\mu\text{g/ml}$ for the sonicated, centrifuged and filtered SWCNT-P; 152, 52, 31 $\mu\text{g/ml}$ for the sonicated, centrifuged and filtered SWCNT-NH₂; 234, 126, 98 $\mu\text{g/ml}$ for the sonicated, centrifuged and filtered SWCNT-COOH dispersions, respectively.

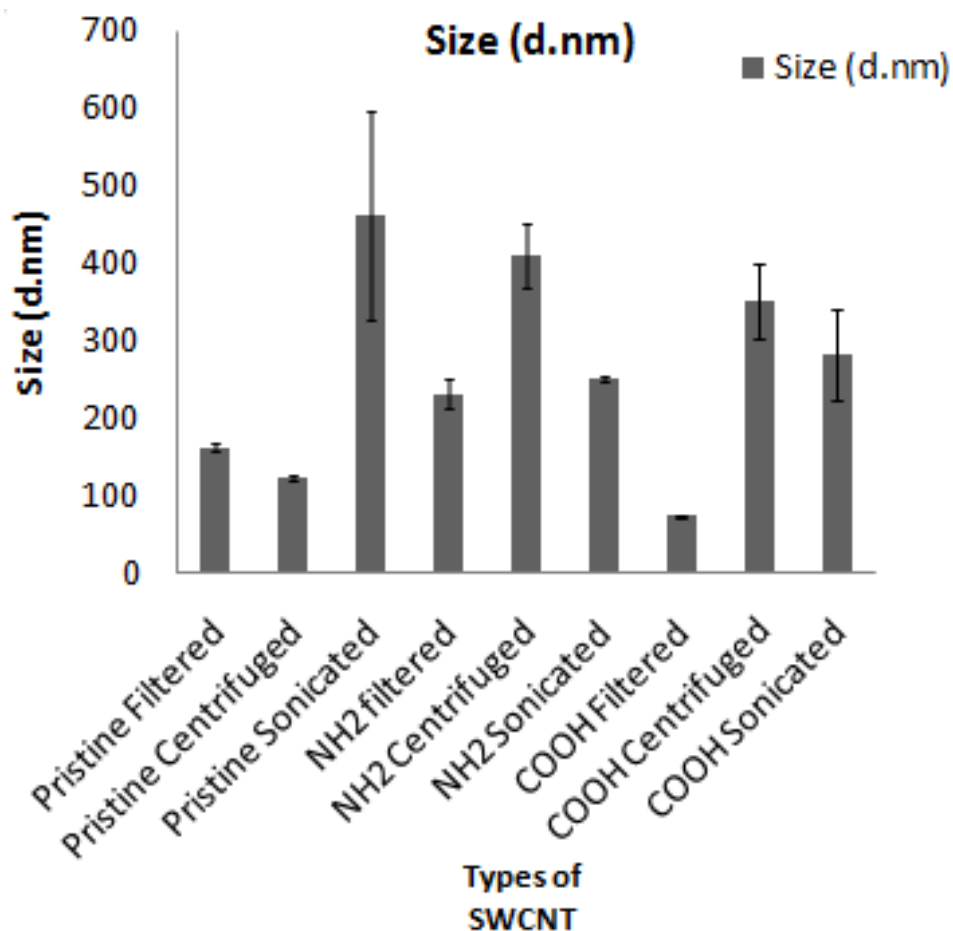


Figure 5.4.2.: Comparison of different types of SWCNTs on the base of filtration, centrifugation and sonication.

The size of SWCNT-NH₂ is measured in 1x PCR Buffer at the range of 25°C and 95°C to observe the relative hydrodynamic size changes when temperature has been changed. Between 25°C and 95°C is chosen because this range includes the thermal cycler temperature changes. According to the data that are obtained from DLS for temperature dependent size change shows that size is increased at the high temperatures however this

increase is not even. It can be said that SWCNTs are not stable and they have tendency to agglomerate but they are not stable in the solution.

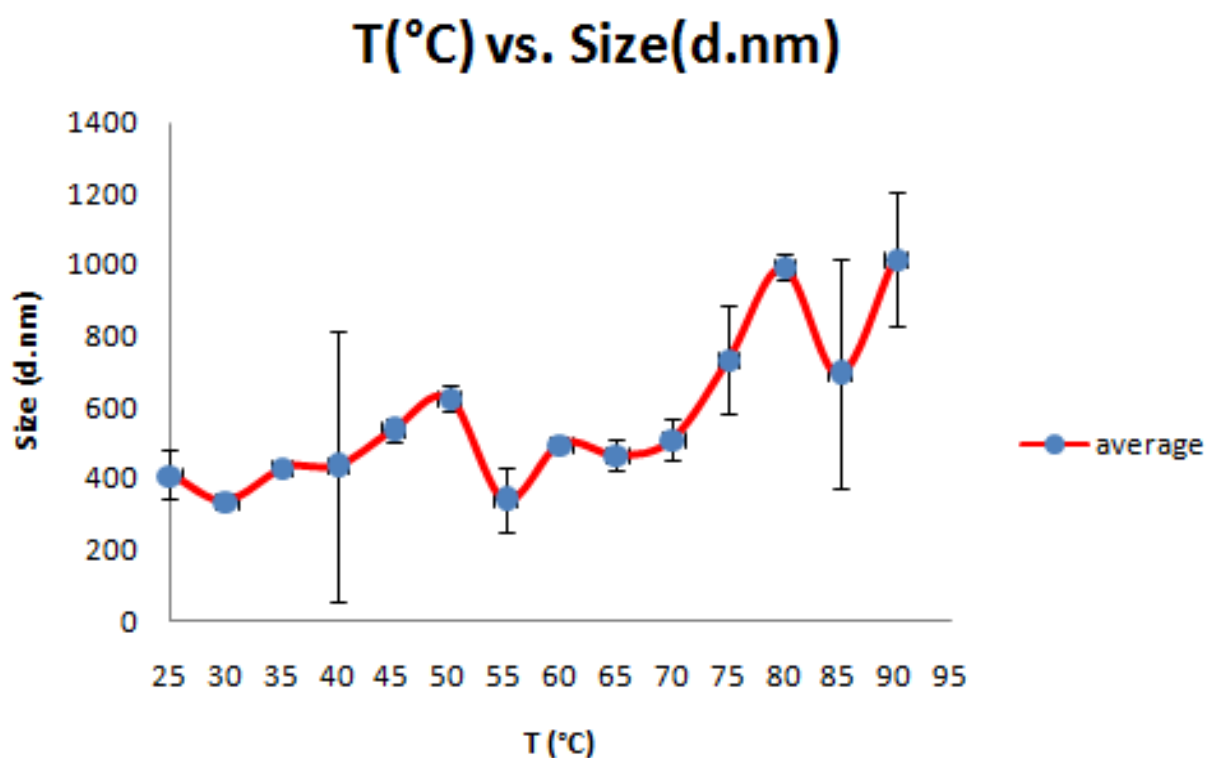


Figure 5.4.3.: Size changes of SWCNT-NH₂ with change of temperature.

To understand that whether template is bind to SWCNTs with the temperature changes, we incubate SWCNT and template for DLS measurements. The temperature change range is from 25 °C to 95 °C that includes the temperature points as PCR have. According to the data, it can be said that SWCNTs have bind to templates because with increasing temperature, size is also increases.

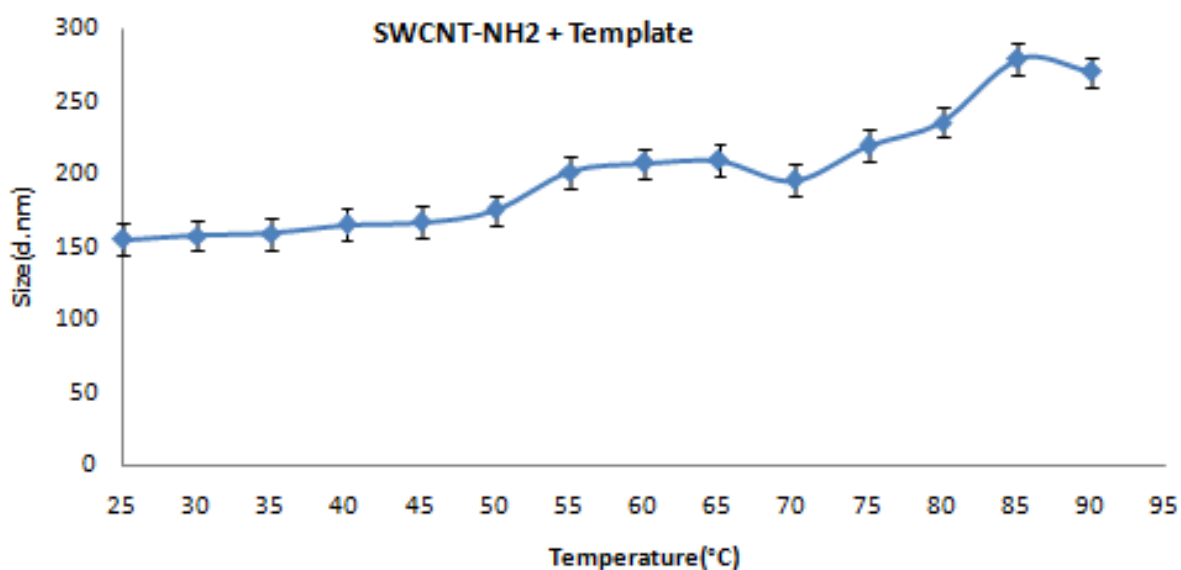


Figure 5.4.4. : The size changes of SWCNT-NH₂ in the presence of template.

To compare the sizes of SWCNTs and SWCNTs and template incubated sample, both graphs are plotted together. The graph shows that SWCNT with template have smaller sizes in comparison to SWCNTs which can be explained as when there is only SWCNT-NH₂, they can bind each other and agglomerate. On the other hand, in the presence of template there is tendency to bind template for individual SWNCT-NH₂ because NH₂ is positively charged and DNA is negatively charged. Thus, there is more tendency to bind between negatively charged DNA and positively charged NH₂.

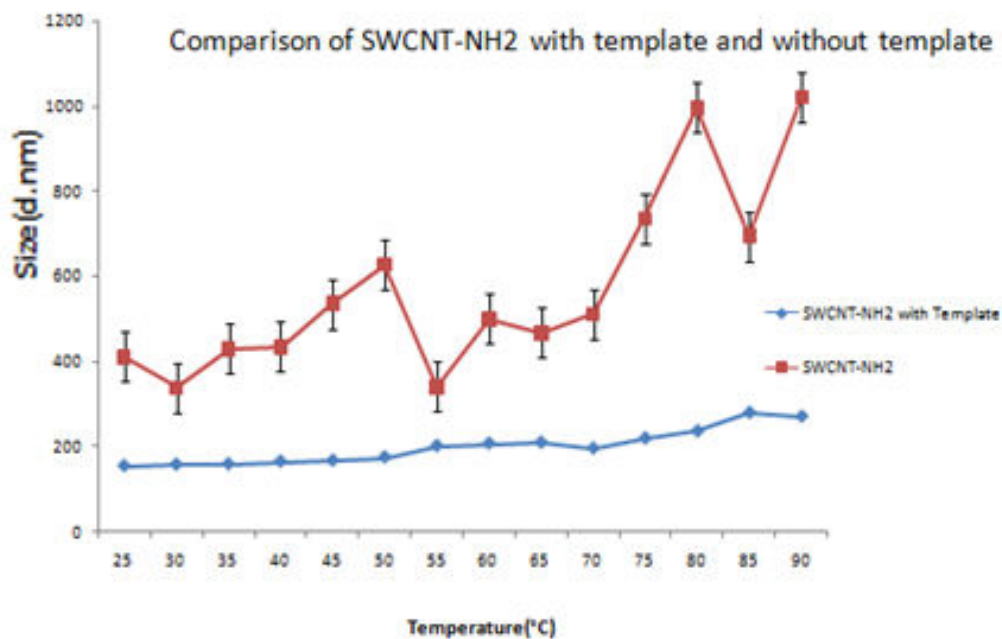


Figure 5.4.5. : The size comparison of SWCNT-NH₂ with and without template.

5.5. Polimerase Chain Reaction and Polyacrylamide Gel Electrophoresis

PCR is performed with pristine, SWCNT-NH₂ and SWCNT-COOH as sonicated, centrifuged and filtered to understand their impacts. SWCNTs are added in PCR tube firstly and serial dilution with 1:1 ratio is performed to observe the difference that based on concentration which are seen on the table. At the end the master mix of PCR is added on the SWNTs. Master mix is added as a drop on the surface of PCR tube and they are scrolled down at the same time with all of them to eliminate the possibility of binding of components before PCR. The components of PCR and serial dilution of SWCNTs are seen on the table

below. After PCR tubes are prepared, thermal cycle is performed and the program is seen on the table.

PCR (25 μ l total)	
10x KAPA Taq Buffer A	2.5 μ l
dNTP(10mM)	0.5 μ l
Forward Primer(165.4 ng/ μ l)	0.25 μ l
Reverse Primer (60 ng/ μ l)	0.25 μ l
MgCl ₂ (25mM)	1 μ l
KAPA Taq Wild Type Enzyme	0.25 μ l
Template(30ng/ μ l)	0.5 μ l

Table 5.5.1.: The components of PCR

Thermal Cycle (Number of cycle : 8)

Temperature	Time duration
95 °C	3 minutes
95 °C	20 seconds
58 °C	20 seconds
72 °C	20 seconds
72 °C	1 minutes

Table 5.5.2.: The program of thermal cycler

Eppendorf Name	Concentration of SWCNTs
1	0.003 mg/ml
2	0.007 mg/ml
3	0.015 mg/ml
4	0.031 mg/ml
5	0.062 mg/ml
6	0.125 mg/ml
7	0.25 mg/ml
8	0.5 mg/ml
9	1 mg/ml

Table 5.5.3. : The concentration of SWCNTs in PCR tube that is prepared by serial dilution

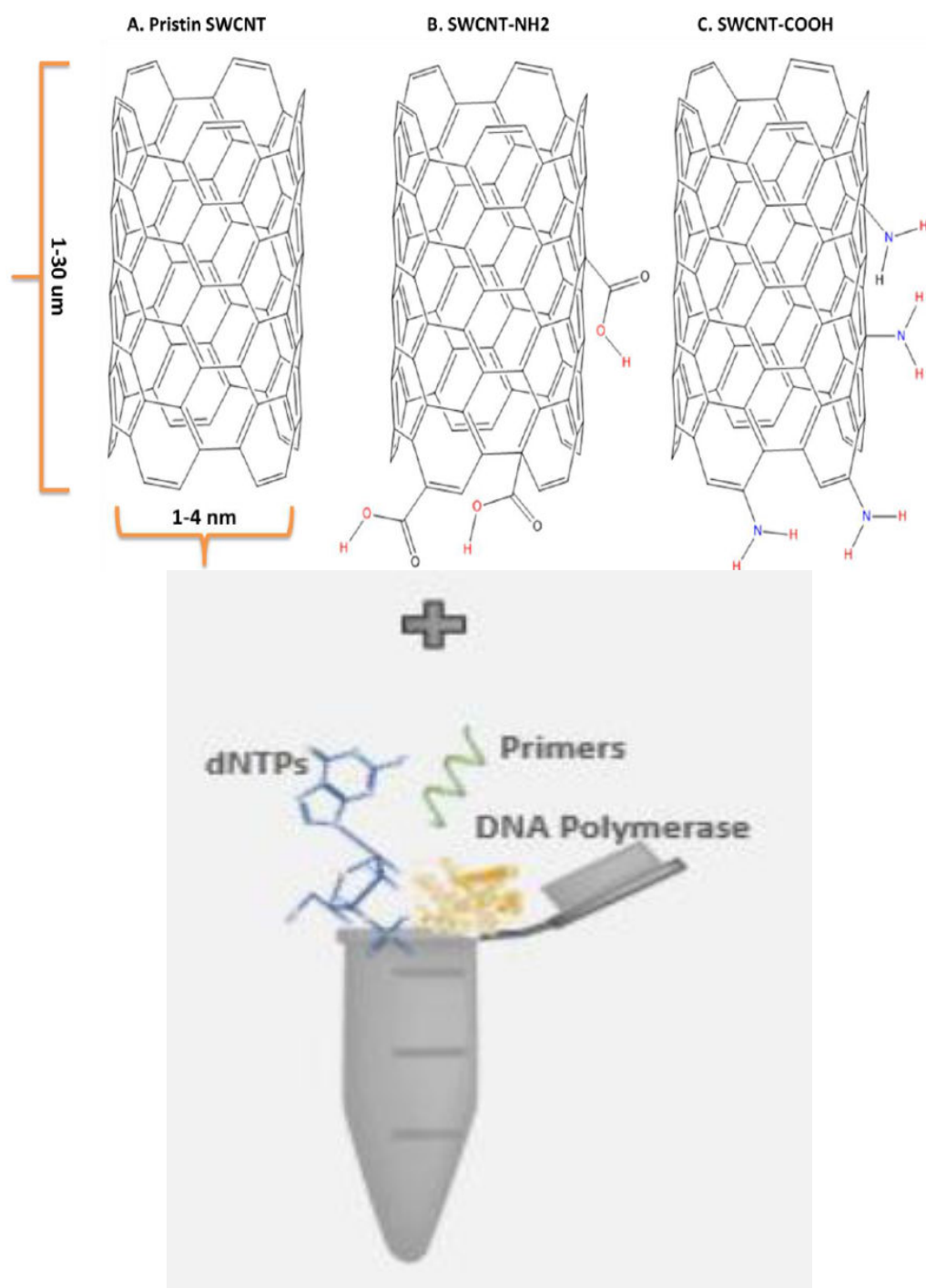


Figure 5.5.1 : Nano PCR with SWCNTs are used as PCR enhancers.

The filtered, centrifuged and sonicated SWCNTs are loaded on the gels at the different concentrations. According to gel images, it is observed that for pristine at the higher concentration for sonicated SWCNTs the reaction have been inhibited. On the other hand, filtered and centrifuged SWCNTs have better results in comparison to the sonicated ones at the higher concentrations. All of SWCNTs are used at the optimum concentration of 1 mg/ml which are dispersed in Milli-Q water including 1% Tween20. According to gel images, it can be seen that at different concentrations all kinds of SWCNTs have various efficiency on PCR.

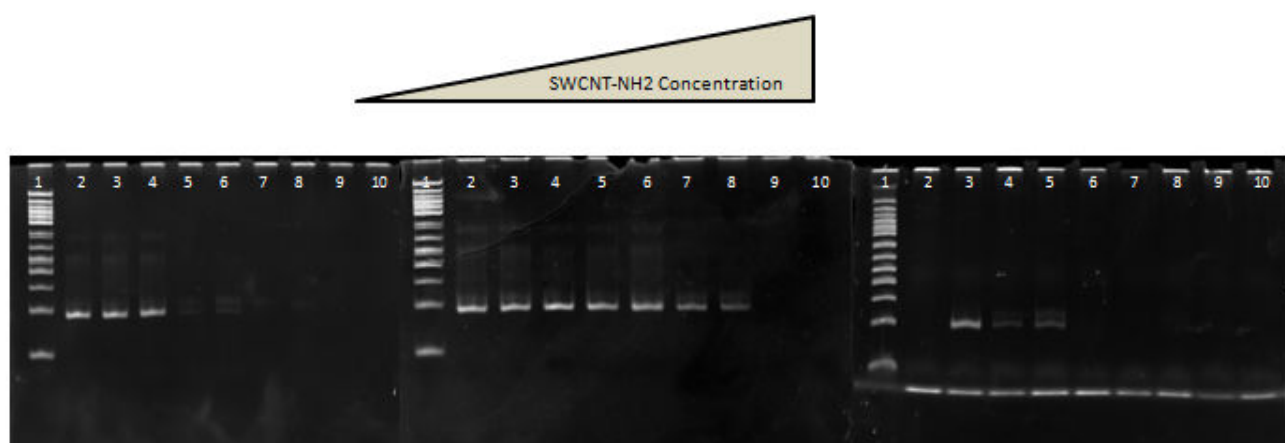


Figure 5.5.2 : From left to right, the images are for filtered, centrifuged and sonicated SWCNT-NH₂ at the maximum concentration of 1 mg/ml including 1% Tween20. First lane is 100bp DNA Ladder. Lane 1 is for 1 mg/ml and the others are serial dilutes as the ratio of 1:1 from the lane 10 to lane 2.

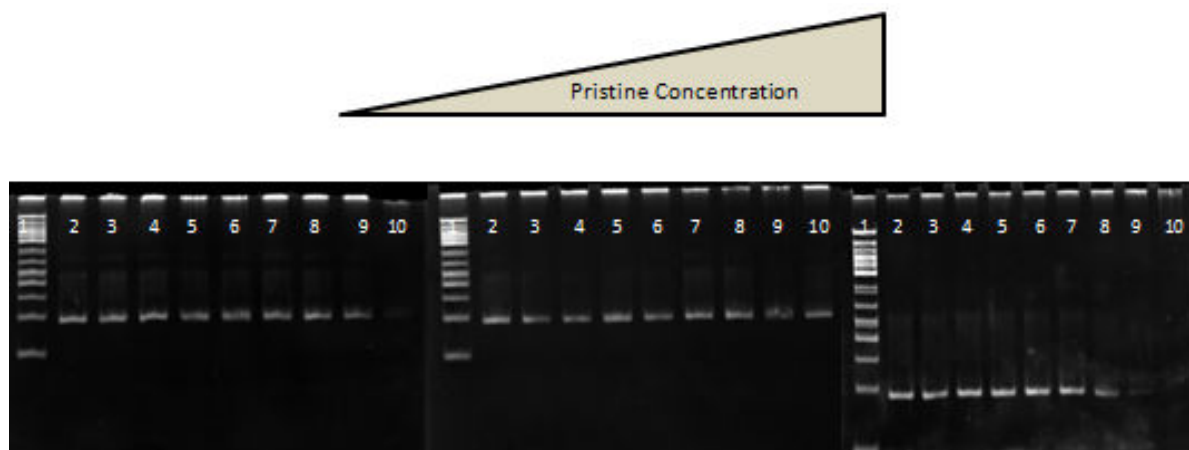


Figure 5.5.3.: From left to right, the images are for filtered, centrifuged and sonicated Pristine at the maximum concentration of 1 mg/ml including 1% Tween20. First lane is 100bp DNA Ladder. Lane 1 is for 1 mg/ml and the others are serial dilutes as the ratio of 1:1 from the lane 10 to lane 2.

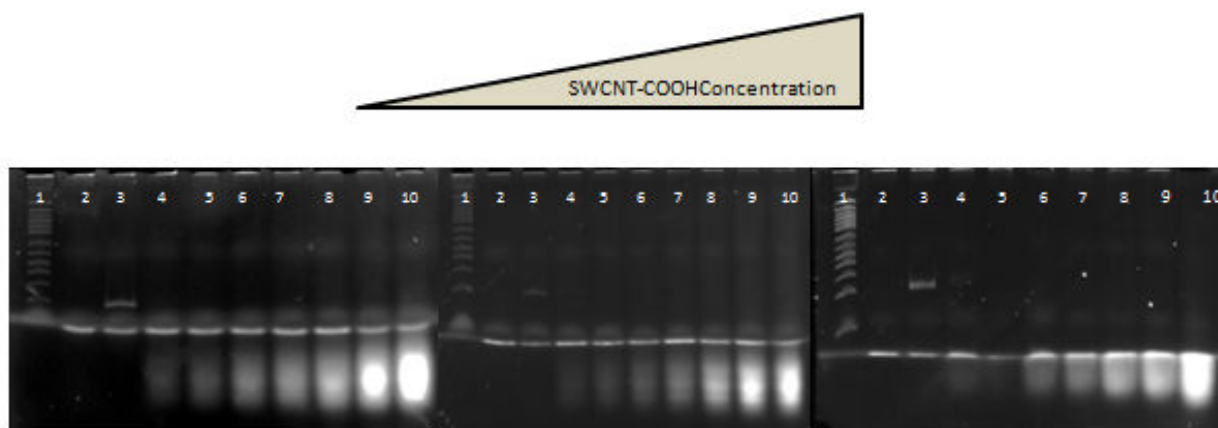


Figure 5.5.4. :From left to right, the images are for filtered, centrifuged and sonicated SWCNT-COOH at the maximum concentration of 1 mg/ml including 1% Tween20. First lane is 100bp DNA Ladder. Lane 1 is for 1 mg/ml and the others are serial dilutes as the ratio of 1:1 from the lane 10 to lane.

6. Discussion

There are many studies on the literature about carbon nanotubes in the context of their impacts on PCR as PCR enhancers which can be acted as Mg^{+2} . PCR enhancers improve the efficiency and specificity of final PCR product and recently nanomaterials are used as PCR additives which is termed as nano additives. For the first time Cui et al. presented that there is a possibility of binding between CNTs and DNA polymerase and that binding can increase the activity and stability of the enzyme.⁵⁶ Thus, addition of CNTs can be effective due to their ability for enhancing the activity of polymerase enzyme.

On the other hand, Yi et. al proved that the activity of Taq polymerase enzyme is inhibited by CNTs.⁵⁷ In addition to that, it was found that CNTs can bind spontaneously to the PCR components that can be the reason of the inhibition of the reaction.¹⁶ SWCNTs interaction with PCR components have a correlation with their dispersion. Filtered SWCNTs are individual and short nanotubes on the other hand sonicated SWCNTs have agglomerated. To minimize the interaction tendency of SWCNTs with PCR reagents, removing the agglomerated SWCNTs is an effective way as it is explained in that work. To understand the interaction between SWCNTs and reagents of PCR, individually all of the reagents should be observed with SWCNT as an interaction.

At higher concentrations, well-dispersed short SWCNTs are resulted lower PCR efficiency. The reason of that result can be thermal conductivity of the PCR solution via SWCNTs that is resulted as effective thermal conductivity. Thermal conditions have impacts on efficiency of PCR and PCR is temperature based reaction. The networking of SWCNTs can be built because of high effective thermal conductivity of SWCNTs. To improve PCR, hot start PCR with well dispersed CNT can be effective.

As a result of work, it is clear that SWCNTs have impacts on PCR positively and negatively. All the findings show that utilization of SWCNTs in biological applications have an aim as enhancement of PCR. In many reports, CNT bundles and aggregations are founded that they inhibit the reaction. Thus, more work is needed to understand clearly the effects of bundles and agglomerations on PCR.

The other following work should explain the binding interactions between CNTs and PCR components as template, polymerase enzyme and primers. To understand putative interactions between CNTs and major PCR components, bead assay can be performed with MWCNTs and magnetic microspheres. OnYuce's work bead assay is experienced with MWCNTs and modified magnetic beads to investigate the possible interactions of MWCNTs and PCR components and demonstrate that DNA template, primers and Taq Polymerase enzyme have an ability to attach on the surfaces of MWCNTs with different tendencies.⁵⁸

7. Future Perspectives

This work could be useful for the further studies that are focused on exploitation of SWCNTs in biological systems for nanobiology, nanomedicine and biosensing. On the ground of the findings about usage of CNTs both MWCNTs and SWCNTs as PCR enhancers enhance the specificity of PCR with a compromised yield. The mechanisms of carbon nanotube-assisted PCR is still obscure. There are already some unknown evidence about interaction between CNTs and major PCR components. There are possibilities about different nanoparticles can display different impacts at various concentrations.

According to literature, there are many evidences that is about different polymerase enzyme and different PCR models as long PCR, GC rich templates and so on can be affected different from addition of CNTs. These variations can affect on biochemical reactions which is critical for future applications of nanomaterials.

Whether the appropriate concentration and nanomaterial is determined, PCR can be improved for obtaining high qualified and high amount of desired product. In addition to that, there is a possibility for eliminating PCR optimization step in the presence of nanomaterials.

To sum up, various nanomaterials give a new insight and opportunities for developing PCR that is the most significant and most used method in molecular biology for numerous of applications. Varied PCR systems as GC-rich template amplification, long fragmented DNA amplification and multiple rounded PCR amplification needs to have superior results and in these kind of PCRs there are many difficulties are faced with. To eliminate these difficulties and obtain high qualified results, nanomaterial-assited PCR should be well improved. NanoPCR is promising application in the most biology and biomedical studies.

For the further researches in this fied, scientists can design nano additives for PCR that can used for one single reactions, fabricate PCR tubes and PCR plates that are covered with

nano additives, fabricate thermal cyclers that are appropriate for nanoadditives. Thus, PCR applications can be addressed in a cost-effective, simple and time-effective manner that can be significant for many research areas as biology and medical.

8. Conclusion

Carbon Nanotubes have attracted by researchers due to their unique electronic, thermal, optical and mechanical properties.⁵⁹ These unique properties make CNTs promising materials for many applications. Nanobiotechnology emerges with integration of biological techniques and nanomaterials.

There are many problems faced with PCR amplification as obtaining nonspecific by-products, low final yield and complexity of GC rich and long genomic DNA amplification. In order to eliminate and minimize these problems, PCR is supported with nanomaterials. A novel area is developed which is based on obtain superior amplification PCR products, is termed as nanoPCR.¹² NanoPCR has difference from conventional PCR as introducing nanomaterials into PCR components. NanoPCR is developed because amplifying low copy number of DNA is essential for many applications. The main benefits of NanoPCR are increased final yield and higher specificity of the target product.

In our work, different types of single-walled carbon nanotubes as pristine, amine functionalized, carboxyl functionalized are used as PCR enhancers. For carbon nanotubes, agglomeration is the most common challenge that must be eliminated to have quality PCR product. Here, we showed that the impacts of pristine, SWCNT-NH₂ and SWCNT-COOH as sonicated, centrifuged and filtered on PCR. All of them experienced at different concentrations. Our data shows that SWCNTs can agglomerate immediately and at the higher concentration, they make huge agglomeration that inhibits the reaction. The data show that the amount of huge aggregates can be eliminated by centrifugation and filtration can make PCR more efficient at the optimum concentration. In addition to that, our result shows that successful amplification of random DNA library with SWCNTs is not dependent to sequence of the target DNA. This finding is similar to Gigliotti's finding which is about long genomic

single stranded random DNA is amplified with disperse CNTs and CNTs efficiently worked.⁶⁰

In conclusion, carbon nanotube-assisted PCR is promising application in various biological studies. The significant information that is obtained from this work is SWCNTs have a great tendency to agglomerate in a while. Thus, big agglomerated SWCNTs should be eliminated to have qualified results.

9. References

1. R. Saiki, D. Gelfand, S. Stoffel, S. Scharf, R. Higuchi, G. Horn, K. Mullis, and H. Erlich, *Angew. Chemie Int. Ed. English*, 1994, **33**, 1201–1207.
2. K. B. Mullis, *Angew. Chemie Int. Ed. English*, 1994, **33**, 1209–1213.
3. S. J. Meltzer, *PCR in Bioanalysis*, Humana Press, New Jersey, 1998, vol. 92.
4. N. Zou, S. Ditty, B. Li, and S.-C. Lo, *Biotechniques*, 2003, **35**, 758–60, 762–5.
5. B. C. Delidow, J. P. Lynch, J. J. Peluso, and B. A. White, *Methods Mol. Biol.*, 1993, **15**, 1–29.
6. D. H. Persing, *J. Clin. Microbiol.*, 1991, **29**, 1281–1285.
7. M. P. Sherman, G. D. Ehrlich, J. F. Ferrer, J. J. Sninsky, R. Zandomeni, N. L. Dock, and B. Poiesz, *J. Clin. Microbiol.*, 1992, **30**, 185–91.
8. C. M. Nagamine, K. Chan, and Y. F. Lau, *Am. J. Hum. Genet.*, 1989, **45**, 337–339.
9. S. Yang and R. E. Rothman, *Lancet Infect. Dis.*, 2004, **4**, 337–348.
10. K. Kasai, Y. Nakamura, and R. White, *J. Forensic Sci.*, 1990, **35**, 1196–1200.
11. R. Gao, A. H. Zhao, Y. Du, W. T. Ho, X. Fu, and Z. J. Zhao, *Blood Cancer J.*, 2012, **2**, e56.
12. H. Nie, Z. Yang, S. Huang, Z. Wu, H. Wang, R. Yu, and J. Jiang, *Small*, 2012, **8**, 1407–14.
13. R. M. Williams, S. Nayeem, B. D. Dolash, and L. J. Sooter, *PLoS One*, 2014, **9**, e94117.
14. D. Cui, F. Tian, Y. Kong, I. Titushikin, and H. Gao, *Nanotechnology*, 2004, **15**, 154–157.
15. C. Yi, C.-C. Fong, W. Chen, S. Qi, C.-H. Tzang, S.-T. Lee, and M. Yang, *Nanotechnology*, 2007, **18**, 025102.
16. Z. Zhang, C. Shen, M. Wang, H. Han, and X. Cao, *Biotechniques*, 2008, **44**, 537–545.
17. X. Cao, J. Chen, S. Wen, C. Peng, M. Shen, and X. Shi, *Nanoscale*, 2011, **3**, 1741–1747.
18. W. Tong, X. Cao, S. Wen, R. Guo, M. Shen, J. Wang, and X. Shi, *Int. J. Nanomedicine*, 2012, **7**, 1069–1078.

19. M. Quaglio, S. Bianco, R. Castagna, M. Cocuzza, and C. F. Pirri, *Microelectron. Eng.*, 2011, **88**, 1860–1863.
20. W. Yang, K. R. Ratinac, S. P. Ringer, P. Thordarson, J. J. Gooding, and F. Braet, *Angew. Chem. Int. Ed. Engl.*, 2010, **49**, 2114–2138.
21. A. K. Geim and K. S. Novoselov, *Nat. Mater.*, 2007, **6**, 183–191.
22. J. Z. Liao and M. J. Tan, *Adv. Mater. Res.*, 2012, **500**, 651–656.
23. S. Iijima and T. Ichihashi, *Nature*, 1993, **363**, 603–605.
24. G. Che, B. B. Lakshmi, E. R. Fisher, and C. R. Martin, *Nature*, 1998, **393**, 346–349.
25. W. A. de Heer, A. Chetelain, D. Ugarte, A. Ch telain, and D. Ugarte, *Science (80-.)*, 1995, **270**, 1179–1180.
26. C. Staii, A. T. Johnson, M. Chen, and A. Gelperin, *Nano Lett.*, 2005, **5**, 1774–8.
27. H. Dai, J. H. Hafner, A. G. Rinzler, D. T. Colbert, and R. E. Smalley, *Nature*, 1996, **384**, 147–150.
28. L. Minati, V. Antonini, M. Dalla Serra, and G. Speranza, *Langmuir*, 2012, **28**, 15900–15906.
29. M. Zheng, A. Jagota, E. D. Semke, B. A. Diner, R. S. McLean, S. R. Lustig, R. E. Richardson, and N. G. Tassi, *Nat. Mater.*, 2003, **2**, 338–42.
30. C. R. Martin and P. Kohli, *Nat. Rev. Drug Discov.*, 2003, **2**, 29–37.
31. H. R. Marsden, L. Gabrielli, and A. Kros, *Polym. Chem.*, 2010, **1**, 1512–1518.
32. G. M. Whitesides and M. Boncheva, *Proc. Natl. Acad. Sci. U. S. A.*, 2002, **99**, 4769–4774.
33. C. Shen, W. Yang, Q. Ji, H. Maki, A. Dong, and Z. Zhang, *Nanotechnology*, 2009, **20**, 455103.
34. J. Hone, M. Whitney, C. Piskoti, and A. Zettl, *Phys. Rev. B*, 1999, **59**, R2514–R2516.
35. A. K. Hu, G. A. Steele, B. Witkamp, M. Poot, L. P. Kouwenhoven, H. S. J. Van Der Zant, A. K. Hüttel, H. S. J. van der Zant, G. A. Steele, B. Witkamp, M. Poot, L. P. Kouwenhoven, H. S. J. van der Zant, A. K. Hu, G. A. Steele, B. Witkamp, M. Poot, L. P. Kouwenhoven, H. S. J. Van Der Zant, A. K. Hüttel, and H. S. J. van der Zant, *Nano Lett.*, 2009, **9**, 2547–2552.
36. M. Fujii, X. Zhang, H. Xie, H. Ago, K. Takahashi, T. Ikuta, H. Abe, and T. Shimizu, *Phys. Rev. Lett.*, 2005, **95**, 65502.

37. M. L. V. Ramires, C. A. Nieto de Castro, Y. Nagasaka, A. Nagashima, M. J. Assael, and W. A. Wakeham, *J. Phys. Chem. Ref. Data*, 1995, **24**, 1377–1381.
38. S. Kang, M. Herzberg, D. F. Rodrigues, and M. Elimelech, *Langmuir*, 2008, **24**, 6409–6413.
39. I. Fenoglio, M. Tomatis, D. Lison, J. Muller, A. Fonseca, J. B. Nagy, and B. Fubini, *Free Radic. Biol. Med.*, 2006, **40**, 1227–33.
40. C. Arndt, S. Koristka, H. Bartsch, and M. Bachmann, *Methods Mol. Biol.*, 2012, **869**, 49–53.
41. L. Dumée, K. Sears, J. Schütz, N. Finn, M. Duke, and S. Gray, *Nanomaterials*, 2013, **3**, 70–85.
42. B. Krause, M. Mende, P. Pötschke, and G. Petzold, *Carbon N. Y.*, 2010, **48**, 2746–2754.
43. H. Isobe, T. Tanaka, R. Maeda, E. Noiri, N. Solin, M. Yudasaka, S. Iijima, and E. Nakamura, *Angew. Chemie*, 2006, **118**, 6828–6832.
44. Y. K. Moon, J. K. Lee, T. K. Kim, and S. H. Kim, *Langmuir*, 2009, **25**, 1739–43.
45. L. F. Pease, D.-H. Tsai, J. A. Fagan, B. J. Bauer, R. A. Zangmeister, M. J. Tarlov, and M. R. Zachariah, *Small*, 2009, **5**, 2894–901.
46. N. Nair, W.-J. W. W.-J. J. Kim, R. D. Braatz, and M. S. Strano, *Langmuir*, 2008, **24**, 1790–5.
47. M. V Ivanova, C. Lamprecht, M. J. Loureiro, J. T. Huzil, and M. Foldvari, *Int. J. Nanomedicine*, 2012, **7**, 403–15.
48. A. Ansón-Casaos, J. M. González-Domínguez, I. Lafragüeta, J. A. Carrodegua, and M. T. Martínez, *Carbon N. Y.*, 2014, **66**, 105–118.
49. B. Zhao, H. Hu, A. Yu, D. Perea, and R. C. Haddon, *J. Am. Chem. Soc.*, 2005, **127**, 8197–203.
50. L. Girifalco, M. Hodak, and R. Lee, *Phys. Rev. B*, 2000, **62**, 13104–13110.
51. L. M. Pasquini, S. M. Hashmi, T. J. Sommer, M. Elimelech, and J. B. Zimmerman, *Environ. Sci. Technol.*, 2012, **46**, 6297–305.
52. T. Dorfmueller, *Berichte der Bunsengesellschaft für Phys. Chemie*, 1987, **91**, 498–499.
53. N. Nair, W.-J. Kim, R. D. Braatz, and M. S. Strano, *Langmuir*, 2008, **24**, 1790–5.

54. H. Isobe, T. Tanaka, R. Maeda, E. Noiri, N. Solin, M. Yudasaka, S. Iijima, and E. Nakamura, *Angew. Chemie*, 2006, **118**, 6828–6832.
55. L. Dumée, K. Sears, J. Schütz, N. Finn, M. Duke, and S. Gray, *Nanomaterials*, 2013, **3**, 70–85.
56. D. Cui, F. Tian, Y. Kong, I. Titushikin, and H. Gao, *Nanotechnology*, 2004, **15**, 154–157.
57. C. Yi, C.-C. Fong, W. Chen, S. Qi, C.-H. Tzang, S.-T. Lee, and M. Yang, *Nanotechnology*, 2007, **18**, 025102.
58. M. Yuce, H. Kurt, V. R. S. S. S. Mokkaapati, and H. Budak, *RSC Adv.*, 2014, **4**, 36800.
59. R. Rastogi, R. Kaushal, S. K. K. Tripathi, A. L. Sharma, I. Kaur, and L. M. Bharadwaj, *J. Colloid Interface Sci.*, 2008, **328**, 421–8.
60. B. Gigliotti, B. Sakizzie, D. S. Bethune, R. M. Shelby, and J. N. Cha, *Nano Lett.*, 2006, **6**, 159–164.